September 2004 ECN-C--04-054

THE INFLUENCE OF FUEL COMPOSITION ON AGGLOMERATION BEHAVIOUR IN FLUIDISED-BED COMBUSTION

H.J.M. Visser

Revisions		
A		
B		
Made by: H.J.M. Visser	Approved/Issued by: H.J. Veringa	ECN Biomass
Checked by: J.H.A. Kiel		

Acknowledgement/Preface

This report describes the results of the project “Influence of fuel composition on agglomeration behaviour in fluidised-bed combustion/gasification of biomass” (contract number 2020-01-12-14-006), conducted in the framework of the Novem subsidy programme Renewable Energy in the Netherlands (Duurzame Energie Nederland, DEN). Novem (currently SenterNovem) is an agency of the Netherlands Ministry of Economic Affairs. The ECN project number was 7.2258.

Essent Energy Production is kindly acknowledged for their financial support, for providing fuel and bed material samples and for their stimulating discussions.

Keywords

Biomass, fluidised-bed combustion, agglomeration, coating development, chemical-physical model, agglomeration indicator

Abstract

In (bubbling) fluidised-bed combustion and gasification of biomass, several potential problems are associated with the inorganic components of the fuel. A major problem area is de-fluidisation due to bed agglomeration. The most common process leading to de-fluidisation in commercial-scale installations is “coating-induced” agglomeration. During normal operation, a coating is formed on the surface of bed material grains and at certain critical conditions (e.g., coating thickness or temperature) sintering of the coatings initiates the agglomeration. This report describes the results of a fundamental, experimental study on the mechanisms of coating formation with time and the resulting de-fluidisation. Bed material samples obtained from both lab-scale fluidised-bed combustion tests as well as from the 80 MWth fluidised-bed combustor of Essent Energy Production in Cuijk (the Netherlands) were examined extensively by Sacnning Electron Microscopy coupled with Energy-Dispersive X-Ray diffraction (SEM/EDX). It appears that the lab-scale combustion experiments enable an accurate prediction of the *initial* processes in coating build-up and the associated agglomeration potential in the full-scale plant. The lab-scale and full-scale samples show a similar coating build-up, but the average coating thickness is much larger for the commercial-scale samples. For all the investigated combinations of woody fuels (and mixtures of 75% woody fuels and 25% cocoa bean or olive stone pulp) with quartz sand, two common types of coatings can be recognised. For the different fuels, only the fraction of the two coating types differs. The coating development, both in terms of morphology and chemistry, appears to follow the same paths. The coating thickness increases with time and with increasing ash content of the fuel. The increase with increasing ash content is less than linear. The impact of the type of bed material appears to be large with olivine showing a chemically different coating build-up. Three agglomeration indicators are proposed, predicting the formation of alkali-silicates on the bed material, the formation of a refractory outer coating and the agglomeration potential due to an alkali-silicate melt phase. In general, the experimental findings are in agreement with the predicted behaviour, but more critical tests have to be conducted to verify the predictive capabilities of the three indicators.

CONTENTS

LIST OF TABLES

LIST OF FIGURES

1. INTRODUCTION

1.1 Background

In (bubbling) fluidised-bed combustion and gasification of biomass, several potential problems are associated with the inorganic components of the fuel. A major problem area is de-fluidisation due to bed agglomeration. In commercial installations, the occurrence of de-fluidisation is still one of the main reasons for unscheduled outages. It damages the image of FBC installations by reducing reliability of electricity production from biomass and, in addition, it negatively influences the investments in future fluidised-bed combustion (FBC) projects. Therefore, it is essential to solve this problem, or at least to bring it under control.

Based on existing knowledge, it is clear that with continuous fuel feeding, de-fluidisation is a self-promoting process. At the onset of bed agglomeration, the fluidisation behaviour gets disturbed due to grain clusters and, as a result, uniform heat distribution is no longer possible. Continuous fuel feeding then leads to local peak temperatures, which promote further bed agglomeration/sintering and de-fluidisation. As a consequence, reactor operation must be stopped to replace the bed material. See Figure 1.1 for a schematic representation of the process. In general, any measures that can avoid unexpected agglomeration or postpone the renewal of bed material are important improvements for commercially operated reactors.

The present study is aimed at contributing to the mechanistic understanding of bed agglomeration/sintering and de-fluidisation in fluidised-bed combustion and gasification of biomass. In order to elucidate under which circumstances agglomeration or de-fluidisation takes place, it is important to study samples typical for the onset of de-fluidisation, i.e. before run-away temperatures induce melting at temperatures higher than those at stable operating conditions. A phenomenon well known and very frustrating for operators of fluidised-bed reactors is, when operation has been stopped due to de-fluidisation and after cooling and removing the bed material no real agglomerates are present or they fall apart into separate grains at the slightest touch. In particular, the mechanisms behind this phenomenon have been studied in detail.

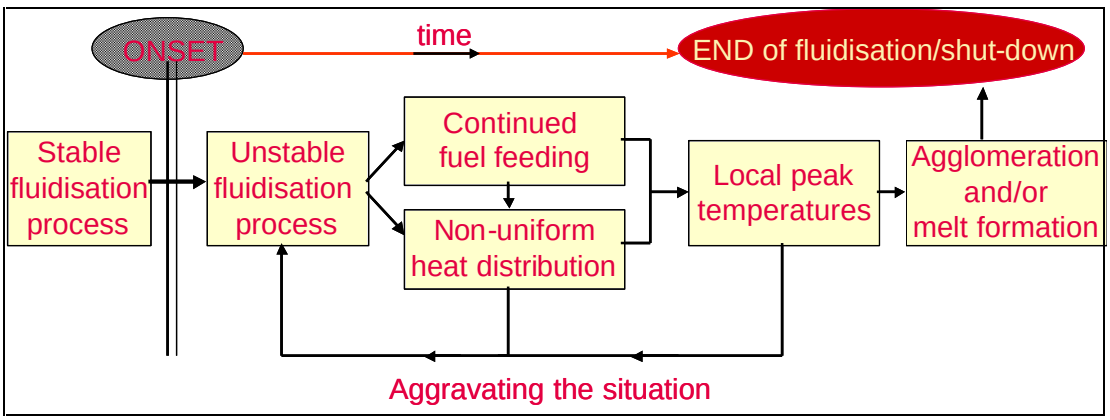

Figure 1.1 *Schematic representation on the processes leading to agglomeration*

1.2 Previous work

During biomass conversion in a fluidised-bed reactor, a large part of the ash leaves the installation as fly ash, while a smaller part remains in the bed. The behaviour of the inorganic ash constituents from the fuel that remain in the bed has been described previously [1,2] based on morphological and chemical analyses of numerous agglomeration samples, obtained from lab-scale to commercial-scale fluidised-bed reactors operated with a wide range of biomass (waste) fuels. From these samples, two extreme types of agglomerates can be identified.

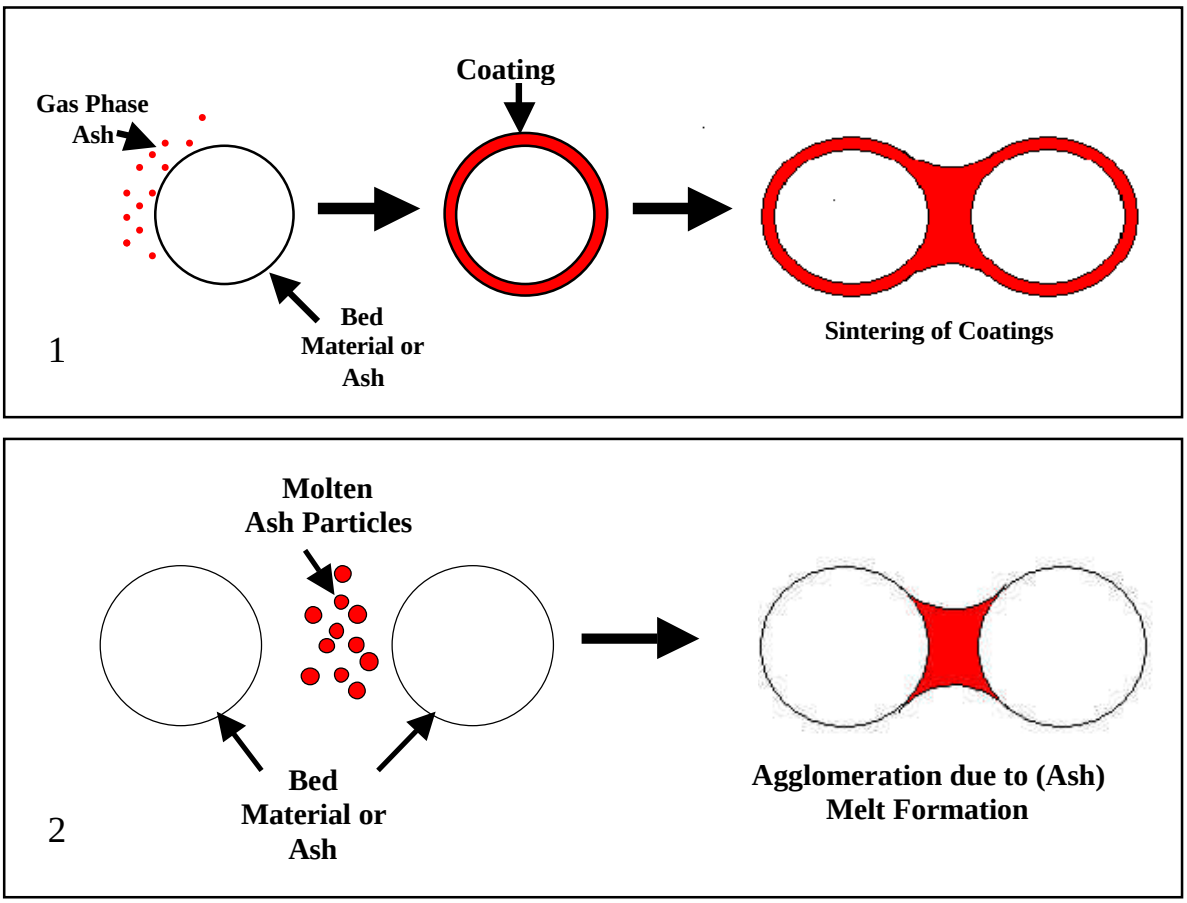

Figure 1.2 *Agglomeration of bed material after coating formation from the gas phase (1) or melt formation of ash components (2)*

One extreme, type (2) in Figure 1.2, results from “melt-induced” agglomeration. In this case, the bed material grains are “glued” together by a melt phase, which roughly matches the chemical composition of the ash and is produced at normal operating temperature. The other extreme type of agglomerates, type (1) in Figure 1.2, is more commonly observed in commercially operated fluidised-bed combustors using woody-type of fuels and results from “coating-induced” agglomeration. Here, a (uniform) coating is formed on the surface of the bed material grains. At certain critical conditions (e.g. coating thickness and/or temperature), neck formation may occur between coatings of individual grains, which initiates the agglomeration. If, however, after first neck formation partial de-fluidisation of the bed leads to local peak temperatures, melt formation may start to take place and a combination of remnants of one extreme and the onset of characteristics of the other extreme may be recognized in one sample. Of the two extreme types of agglomeration illustrated in Figure 1.2, type (1) is found to be the dominant process in most commercial-scale installations. In addition, it is found that de-fluidisation resulting in non-lasting agglomerates upon cooling of the installation, usually involves these types of coated grains. Therefore, the coating-induced type of agglomeration has been studied in more detail.

The presence of a coating layer on bed material grains and the extent to which this phenomenon occurs in a wide variety of fluidised-bed reactors, was acknowledged by the author when large numbers of samples from different test installations (lab-scale to 3 MW pilot-scale) were studied. The samples were studied in the 4th framework EU project "Minimum Emissions" [2] from 1998-2000, in combination with commercial work on bed material from a 80 MW_{th} FBC installation of Essent Energy in Cuijk (the Netherlands) in the same period. The standard procedure for studying bed material samples involved the mounting of the samples in epoxy resin and the subsequent cutting and polishing of the mount to be examined under the Scanning Electron Microscope (SEM). Only when studying the sections of bed material grains became common practice in this period, the commonness of the coating phenomena became apparent.
Based on the knowledge of the common appearance of the coatings and their potential involvement in de-fluidisation, a more basic research program was set up at ECN in 1999, in which the fluidisation behaviour of artificially coated material was studied. The coating consisted of K-silicate evenly distributed on SiO_2 (quartz) or Al_2SiO_5 (mullite) grains via a sol/gel mechanism [3]. One of the main conclusions of this work was that a critical minimum coating thickness of only 1-1.5 μm is in some cases required to induce de-fluidisation [1,3]. Another important conclusion was that de-fluidisation occurred already at temperatures at least 100-150°C below the melting temperature of the coating composition and no indications of a melt phase were observed [1,3].

Because the artificial coating technique limited both the necessary thickness-variation as well as composition, it was decided to continue research in 2000 with coated bed material obtained from biomass Fluidised-bed combustion (FBC) and Fluidised-bed gasification (FBG) experiments performed in the ECN lab-scale fluidised-bed reactor "WOB". The general approach of first creating coated bed material and subsequently testing its fluidisation behaviour in another fluidised-bed test facility was established. This 2-step approach was successful on showing the importance of coating-induced agglomeration [1]. However, the tests were performed on bed material with relatively thin coating layer that was the resultant of 8 hours of combustion/gasification. More insight was gained when the coating thickness and chemical type proved to play a role in the temperature of agglomeration [1]. Samples studied from Cuijk indicated that the coating would most probably evolve with time and the combination of these data resulted in the awareness that the formation of coatings with time could be an important parameter in processes leading to agglomeration and therefore worthwhile to be studied more systematically.

Several other research groups have reported in recent years the common presence of coatings around bed material grains, from lab- to commercial-scale fluidised-bed installations, which indicates that it is a universal feature, not related to just 2 FBC installations producing the samples for this study. Laitinen et al. [4] found the coating thickness to be 2-20 μm on bed material grains using plywood-sawdust mixtures as fuel in a 5 MW Bubbling Fluidised-bed reactor. Lind et al. [5] found that quartz bed material of an industrial scale (35 MW) Circulating FBC contained coating layers using willow and/or forest residue as fuel. The thickness of the coatings was mostly 5-10 μm, up to 50 μm locally. Thickness was concluded to be dependent on sand feed/ bottom ash removal as well as attrition. Öhman et al. [6] found coatings with an average thickness of 10-50 μm on bed material from a 18 MW Circulating Fluidised-bed reactor and from a lab-scale test facility using 8 different fuels.

1.3 Aims

The present study is in general aimed at avoiding/diminishing the outages of commercial-scale fluidised-bed reactors due to bed agglomeration by contributing to the mechanistic understanding of bed agglomeration/sintering and de-fluidisation during combustion and gasification of biomass. In order to elucidate under which circumstances agglomeration or de-fluidisation takes place, it is important to study samples typical for the onset of de-fluidisation, i.e. before run-away temperatures induce melting at temperatures higher than those at stable operating conditions. This requires dedicated tests for agglomeration research only.

More specifically, the aim is to study the coating build-up on bed material grains with time. The dependence of coating growth with time and fuel composition is studied in detail. Once coating compositions with time and the role of the composition in agglomeration processes will become known, bed replacement schedules in commercial plants can be optimised which will improve the economy of the total process.

The fuels and bed materials used in this study have been obtained from Essent Energy Production and have been (are) used in their 80 MW_{th} commercial FBC plant in Cuijk (the Netherlands). By using Cuijk fuel/bed material combinations, the experimentally created, coated bed material can be directly compared with the spent bed material from Cuijk. Operators of the full-scale plant indicate that apparently small differences in the wood streams delivered could be a reason of the occasional agglomeration occurring at this plant. When the laboratory created coating compositions can be considered comparable with those in Cuijk, it is the aim to determine which woody fuel streams in the Cuijk-mix contribute mostly to coating thickness/composition combinations and have the highest potential for agglomeration. In this way, the present study is directly aimed at giving more insight in the mechanisms of agglomeration occurring occasionally in the commercial Cuijk installation.

For the longer term it is aimed to come to more general models that could directly derive the agglomeration potential from fuel/bed material compositions. Because the bed material is first taken to be constant in the present study (quartz sand), the first attempt is directed towards agglomeration indicators to predict the agglomeration potential in combination with quartz sand.

2. APPROACH

2.1 General

In this study the general approach has been as follows. First, to perform extensive fuel analyses using proximate, ultimate and ICP/AES analyses methods in order to characterise the (in)organic content of the fuels used thoroughly. Subsequently, for the Cuijk fuel-mix, the mixtures of the individual fuel streams were calculated and the calculated inorganic element concentrations were compared with the analysed Cuijk-mix (as used in Cuijk). Based on the fuel analyses, agglomeration indicators were calculated per fuel to assess the agglomeration potential beforehand. Next, the fuels were prepared, to be used in the lab-scale fluidised-bed combustion installation (the "WOB") at ECN. The aim was to combust the fuels under conditions as close as possible to those in Cuijk, and to sample the bed material, during and after these tests. The bed material samples were further prepared for study under the Scanning Electron Microscope (SEM). From the chemical and morphological data obtained using the SEM, a first attempt was made to develop conceptual models for the coating build-up during fluidised-bed combustion. A more detailed description of each of the steps in the approach is given below.

2.2 Fuel Analyses Methods

The determination of moisture, volatile matter and ash content in solid fuels is a macro-method known under the name "proximate analysis". The procedures followed at ECN are ISO 589 for the determination of moisture content, ISO 562 for the determination of volatile matter and ISO 1171 for the determination of the ash content at 815^{o}C. Ashing at 550^{o}C is according to the "Dutch best practice method (BPM) for biomass fuel and ash analysis" [7], which is similar to the Swedish norm SS 187171. In general ISO norms are all well established for coal and were adjusted for biomass. The resulting adjustments are according to the national agreed BPM [7]. The analyses of C, H and N are determined in a reaction column at 1030^{o}C. The procedure is also according to Dutch BPM [7] and based on ISO 625 for coal and coke.

The calorific value is determined by adiabatic combustion of the fuel at a pressure of 25 atmospheres in a pressure vessel according to Dutch BPM [7] and following ISO 1928 for solid mineral fuels. The temperature difference before and after combustion is determined and the calorific value in J/g can be calculated. The condensation heat of water is included in the result and the calorific heating value thus determined is the higher heating value, abbreviated as HHV.

Chlorine is determined by activation analysis. With this method total chlorine is determined by radiating the sample with neutrons for 1 minute in the ECN low flux reactor. The gamma-spectrum of chlorine isotope 38 that is formed is recorded and compared with internal standards. The result of the measurement includes both organic and inorganic chlorine and can be considered more complete than analysis following controlled (pressurised) combustion of the fuel.

The inorganic content of the fuels is determined by the Inductively Coupled Plasma/ Atomic Emission Spectroscopy (ICP/AES). AES is a form of analytical spectroscopy that uses atomic spectra in the optical part of the electromagnetic spectrum (ultraviolet, visible light and near infrared). The atomic spectra have their origin in the energy transitions in the outer electron orbits of free atoms and ions. Therefore, the sample material needs to be dissociated into free atoms and ions. For partially organic solid samples, the first step is to dissolve the sample. This is a critical step, because what is not in solution will not be analysed.

At ECN the fuels are not ashed before analyses. This is considerably more accurate for main components as well as trace elements, which evaporate easily at relatively low ashing temperatures. The obtained solution is introduced into the ICP, the inductively coupled plasma, where it is nebulised to aerosols and subsequently led into the plasma-excitation source. The plasma converts the sample material into atomic form as well as increases the energy level of free atoms and ions into an exited form, necessary for the spectroscopy and element analyses. Internal standard solutions are used to make the method quantitative.

2.3 Agglomeration indicators assessing the agglomeration potential

Control of the total bed chemistry (determined by fuel type, bed material and additives) is a common way of minimising "sticky" material formation. As a first approximation, indicators for a high potential in bed agglomeration are distinguished based on "agglomeration indicators" only. Obviously, the chemistry of the fuel only determines part of the total bed chemistry and in previous studies the interaction between fuel ash-components and bed material has been shown to be very important [1] and [3]. The first agglomeration indicators are derived for SiO_2 as bed material and are based on general observations from many previously studied samples.

The first agglomeration indicator is:

$$(Na + K) / (2S + Cl) > 1 \qquad (I1)$$

This indicator, I1, is based on the general observation that the initial gas phase alkali concentration is attributable to the concentration in the fuel, the bed temperature and to the presence of S and Cl which favour gas phase release and binding in relatively volatile compounds at sufficiently high temperatures. Therefore, as a first approximation, it may be assumed that for a high alkali-induced agglomeration potential at temperatures > 800 ^{o}C, the ratio (Na+K)/(2S+Cl) must be larger than 1. This is a broad estimate as it assumes that all the S and Cl present in the fuel reacts with the fuel alkali species and does not take into account:

(a) that a significant proportion of the S and Cl will be released as HCl and SO_2, and
(b) that the presence of other cations will compete to associate with Cl and S.

A second agglomeration indicator for agglomeration is proposed to be:

$$(K + Na + Si) / (Ca + P + Mg) > 1 \qquad (I2)$$

This second indicator, I2, is based on the fact that in previously studied samples, the coating build-up around SiO_2 grains often developed in an inner alkali-silicate reaction rim and an outer rim relatively enriched in Ca, P and Mg. The outer rim composition is definitely of a more refractory composition, therefore has a much higher melting temperature and hence a lower potential to lead to agglomeration. When sufficiently thick and overall present, the outer rim functions as a non-sticky outer layer. A ratio in which (Ca + P + Mg) is larger than (K + Na + Si) from the fuel is thought to have a good potential to form such an outer non-sticky layer. The value of 1 is arbitrary to a large extent, because it is unknown if an equally thick layer of the refractory rim is required to counterbalance the sticky inner layer. The distribution of the elements to form the outer refractory layer into a continuous layer is probably of much greater importance. The above mentioned second agglomeration indicator is new and must be regarded as an hypothesis to be verified/modified by data obtained in this study.

It is proposed for further testing, that both agglomeration indicators, as described above and being larger than 1 predict a high potential of alkali induced agglomeration based on the fuel characteristics in combination with SiO_2 bed material at temperatures > 800 ^{o}C.

2.4 “WOB”-tests and bed material sampling

The “WOB” (see Figure 2.1) is a lab-scale fluidised-bed reactor that can be used in both combustion and gasification mode. In this study only combustion experiments were performed.

Figure 2.1 *Photograph of the lab-scale fluidised-bed installation “WOB” at ECN*

A schematic diagram of the “WOB” is given in Figure 2.2. It is a printed version of the control panel of the computer on which the tests are monitored and controlled.

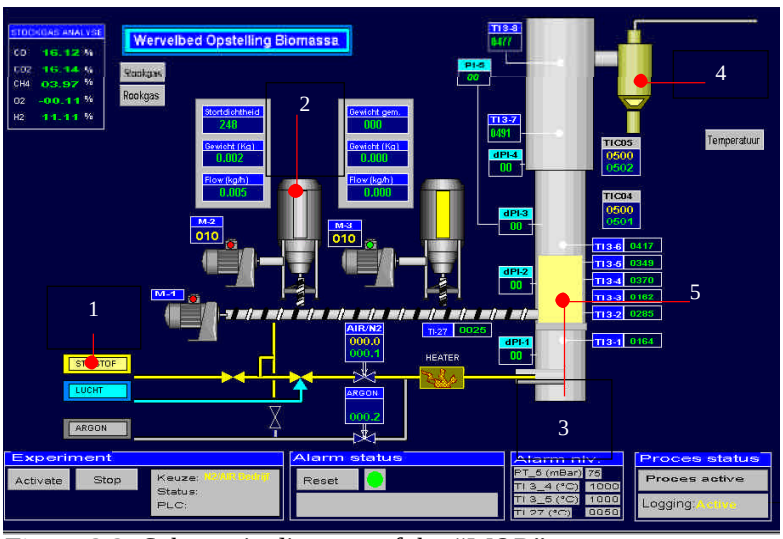

Figure 2.2 *Schematic diagram of the “WOB”-reactor*

The inner diameter of the reactor is 74 mm (at the position of the bed) and widens to 108 mm (at the position of the freeboard). The temperature of the electrically heated reactor wall can be controlled independently of the fuel used and enables the simulation of adiabatic conditions. A

combination of air and nitrogen has been used as the fluidisation medium in all experiments performed. The fuel, typically < 2mm in grain size, is fed to the reactor using a screw feeder. The gas stream passes after the reactor into a cyclone separating ash and gas. The cyclone ash can be sampled and the gas stream is on-line analysed on O_2, CO_2, CO, C_xH_y, NO, NO_2 and SO_2. Further, pressure differences over the bed region as well as five local temperatures within the reactor are monitored.

At the bottom of the bed section, an additional option for sampling bed material has been created. This sampling port allows the discharge of bed material during the tests and has been used to take samples at regular intervals to study the build-up of coatings around the grains. Table 2.1 shows the conditions that were used during the tests performed for this study.

Table 2.1 *Experimental conditions used for the tests in the "WOB"*

Reactor wall temperature top	850 ºC
Reactor wall temperature bottom	850 ºC
Fuel amount	650 g/h
Oxygen level	approx. 6 % (max 11%)
Air	70 l/min
Nitrogen	25 l/min
Nitrogen flow on the fuel feeding	0.5 l\min
Bed material grain size ($d_{p,\ average}$)	Cuijk sand (unused) = 0.8-1.2 mm
Weight of bed material sand	1060 g
Grain size of the fuel particles	0.7 mm < x < 2.0 mm
Type of bottom plate	25x 1mm holes with sand discharge possibility

Experiment duration was between 6 and 16.5 hours depending mainly on the amount of prepared fuel available. Only one combination of fuels and bed material (Cuijk mix with 25% olive stone-pulp and quartz sand) resulted in agglomeration and had to be stopped for this reason. Therefore, it is thought that the coatings developed do in most cases not yet represent the situation at the onset of agglomeration, but are the grain-coating morphology at an earlier stage. Ideally, the coating development should have been followed up to the onset of agglomeration. However, this proved to take much more time than anticipated. Additional information, extrapolating coating development with time, has been obtained from studied Cuijk samples.

The first series of fuels from Cuijk arrived at ECN in May 2002. The material was however, harvested in March/April. In June, pre-treatment by drying/milling/sieving took place. The reason for this pre-treatment is that the maximum grain size that can be fed into the WOB is 2 mm. The first 5 WOB-tests lasted 6-8 hours under stable conditions and the samples were studied under the SEM. Unfortunately, the coating formed on the bed material grains was still very thin and the differences between the samples from different wood fuels were negligible. Therefore it was decided to re-use the bed material in a new series of tests as much as possible and shift the main aim of research more towards the coating build-up in time.

In order to perform the second series of tests, new fuels were asked at Essent. The second series of woody fuels was harvested in August/September. To be on the safe side these were also fully analysed and pre-treated the same way. This second series of tests (6-11) were longer duration tests, in order to allow as much coating build-up as possible. Not only at the end of the tests were bed material samples taken, but also during the tests, continuing reactor operation.

Tests 12 – 14 were carried out with the Cuijk wood-mix as fuel and/or with additional olive stone-pulp and cocoa beans. The aim of these last tests was to get a first impression of the effect on the coating build-up from very different fuels. In addition, a test was performed using olivine

sand as bed material to get a first impression on the effect of coating build-up on different bed material than quartz sand.

2.5 Morphological- and chemical sample investigation by SEM-analyses

After cooling down of the bed material samples, the grains were imbedded in epoxy resin. The blocks of epoxy resin were cut and polished to obtain sections of the bed material grains to be studied further by SEM including the Energy-Dispersive X-Ray (EDX) diffraction for on-line analysis. The total SEM-sample preparation procedure was performed without any water containing ingredients in order to avoid any possibility of (partial) coating dissolution.

Under the SEM, the samples were studied morphologically, to obtain e.g. the average coating thickness, to establish the presence of 1 or more concentric rims (inner/outer/middle layers) and the general mode of coverage of grains by the coating (even distribution/ in big patches). The morphologically recognized features were analysed under the SEM by EDX, which allows point analyses down to 1 μm^3. In this way an extensive dataset per sample was generated on the coatings morphology and chemistry.

2.6 Changes to the original work plan

The total number of WOB-tests as planned (and budgeted) had to be reduced due to the unexpected outcome of the first series of experiments, in which the coating thickness and chemical variation after 8 hours were insufficient to yield useful samples for the development of agglomeration models. This resulted in a less extensive parameter variation than originally planned. This change of plan was communicated with Novem in one of the regular meetings at ECN.

It was agreed that the budget would be directed to longer duration tests in order to obtain more useful samples with more clear coating differences. The emphasis would be shifted from extensive parameter variation between tests to a less extensive parameter variation but longer duration tests that would allow the study of coating build-up with time. As a consequence the construction of agglomeration process-models would also be more directed to the coating build-up with time. Originally foreseen were a number of WOB-tests (of 8 hours duration) to verify the models obtained. It was agreed however, that most of the budget would be used for the series 1 and 2 of WOB-tests as mentioned above in order to obtain useful samples for modelling. Verification of the obtained models by more WOB-tests was eliminated from the project. However, a new type of verification was introduced, namely the comparison of the WOB-samples with samples from the commercial-scale installation in Cuijk, using the same fuels and bed material. Both lab-scale samples and the models derived from these samples (on the coating build-up with time) were verified to occur in practice during longer time operation in a commercial-scale plant.

3. RESULTS

3.1 Fuel analyses

3.1.1 Fuels used in this study

The analyses of the fuels used in this study are given in Appendix 1. The first four are individual streams that make up the regular Cuijk mixture of woody products. The first fuel series obtained is indicated with a 1, the second series with a 2. Next is the Cuijk mix as obtained, already mixed, from the Cuijk plant and for comparison the Cuijk mix as calculated from the contributing individual 4 streams. The last two fuels are olive stone-pulp and cocoa beans, which were considered at Cuijk as secondary fuel in combination with the ordinary Cuijk wood mix. A short description of the 4 fuels that make up the Cuijk mix is given below to understand the different origins of the woody fuels.

- Wood clippings: Mainly from parks and other planted community areas.
- Uprooted forest wood: From areas that are cleared from planting. This material is unsuitable for wood production and hence whole trees are present in this stream.
- Plantation thinning wood. In production forest, thinning of complete small trees is taking place to allow the remainder of the trees to have more growing space. The total trees in this stream are usually young and fast growing.
- Sawdust: white wood. Sawdust from industries processing wood.

Based on the experience that the problem causing elements are often present in larger quantities in leafs, bark and fast growing parts of the plant, the following order in agglomeration potential is considered to apply based on this reasoning (from high to low):

Wood clippings > thinning wood> uprooted trees> sawdust.

It is the same argument that is applied by the operators at Cuijk to keep the fraction of wood clippings limited, despite the most attractive price of all wood streams. It is unknown how the Cuijk mix would fit in the order of agglomeration potential and this is one of the issues to be addressed.

3.1.2 Cuijk mixture and relative contributions from individual wood streams

In Cuijk, a mixture of the above-mentioned wood streams is used as their regular fuel. The relative contributions of the four streams in the mixture are (on a mass base): 10% wood clippings (to be referred to as “clippings”), 6% uprooted forest wood (uprooted trees), 10.5% plantation thinning wood (to be referred to as “thinning wood”) and 73.5% industrial sawdust. With the obtained analyses of the individual fuels, given in Appendix 1, the relative contributions of the individual streams in the mix with respect to the inorganic element concentrations can be calculated and are given in Tables 3.1 and 3.2. Not the absolute numbers but the relative percentages to the mixtures are indicated for ease of comparison.

The aim of the mixture calculations is twofold. On the one hand, the individual streams can be characterised as contributing small/large amounts of the problematic elements. Because the relative weight contribution of one of the individual streams to the mix can be totally different from e.g. the relative contribution of K to the mix. On the other hand the mixtures calculated can be compared with the mixture as received and analysed, to make sure that the relative

contributions of the individual streams are indeed representative of the truly used Cuijk mix. Note that the Cuijk mix calculated is set at 100% and the Cuijk mix analysed is given as a percentage relative to the Cuijk mix calculated.

As can be seen from the Tables 3.1 and 3.2, the differences between the Cuijk mixes as analysed and calculated are reasonably small for the overall ash content as well as for most of the main inorganic elements. This justifies work based on the individual streams to be considered as fraction of the Cuijk mix. An exception is the amount of Si. It seems that the Si calculated in the Cuijk mix is dominated largely by the Si-content of the wood clippings fuel. This stream is known for its large amount of attached sand, which would disturb the Si value obtained from the wood.

3.1.3 Comparison between wood and the other fuels

In general, wood is considered to be one of the most easily used types of biomass in terms of ash content and ash behaviour. It is questionable, therefore, if a commercial FBC plant should consider alternative biomass fuels when designed for wood. With this question in mind, the analyses of the wood type fuels and the other two fuels are compared.

The ash content is with 6 and 5% for olive-stones and cocoa beans, respectively, slightly larger than for the wood fuels of series 1, however, the wood fuels of series 2 contain in some cases much higher ash quantities than the olive-stone and cocoa bean fuels. Nitrogen is higher for the other fuels and oxygen somewhat lower compared to wood. The latter could indicate that fuel–related NO_x could be higher than for wood.

When considering the main inorganics and especially the problematic elements it can be seen that the characteristics of Al and Si are comparable to the description of the total ash content, i.e. the content for the other fuels is higher than in the case of the series 1 wood fuels but smaller than most of the series 2 wood fuels. Chlorine is very high for both olive stone and cocoa bean fuel, while S is very high for cocoa bean and comparable to wood for the olive stones. Na and K are much higher for the two other fuels than for the series 1 wood fuels, however, the concentrations are comparable to some of the series 2 wood fuels. Ca and Mg, finally, are relatively high for the two other fuels compared to wood, but this would be a beneficial feature (see the next Section on agglomeration indicators).

In conclusion, only chlorine and possibly nitrogen seem both relatively high and possibly negative characteristics of the other fuels in comparison to wood. S is high for cocoa beans, but not known beforehand to be a definite negative feature. The higher Ca and Mg of the other fuels could be beneficial; while in general ash content as well as Na plus K contents in the other fuels are intermediate between the series 1 and series 2 wood fuels. Therefore, the other fuels can not be concluded to be more problematic than wood would based on the analyses, and the enormous difference between the series 1 and series 2 wood fuels deserves some more detailed explanation. Considering all problematic elements and total ash content to be higher in the series 2 wood fuels (except maybe for sawdust) compared to series 1, this might lead to the source of fuel variation that is thought to sometimes cause agglomeration unexpectedly. SEM-observations and analyses will provide additional information and are described in Section 3.4.

Table 3.1 *Ash- and elemental contributions of the individual streams to the calculated Cuijk mixture in percentage values for the first series of fuel. 11 = relative concentrations of elements higher than the relative ash-contribution to the mix. 11 = relative concentrations of elements that are lower than the relative ash-contribution to the mix. 11 = the stream that contributes the largest fraction of the element to the mixture*

Fuel	Clippings 1 10%	Uprooted wood 1 6%	Thinning wood 1 10.5%	Sawdust 1 73.5%	Cuijk mix* 1 as analysed	Cuijk mix+ 1 calculated
Ash (at 550°C) as wt% of fuel	0.28	0.11	0.01	0.44	0.94	0.84
Ash (wt% in mix)	33.3	13.1	1.2	52.4	111.9	100
Elements in ash (wt% in mix)						
Cl	4.4	2.3	2.4	90.9	102.0	100
S	20.5	11.8	14.4	53.4	90.3	100
Si	94.3	1.1	0.7	3.9	*9.8*	100
Al	68.3	4.4	6.3	21.0	53.4	100
Na	48.2	9.6	8.3	33.9	66.9	100
K	22.0	10.3	11.7	56.0	94.0	100
Ca	23.9	11.3	10.7	54.0	86.4	100
Mg	22.4	10.5	12.5	54.6	95.4	100
P	21.8	16.1	14.0	48.2	100.0	100
Fe	38.9	6.1	4.9	50.2	94.5	100
M	5.9	3.0	6.3	84.8	118.0	100
Cr	47.1	3.5	6.2	43.2	58.8	100

Table 3.2 *Ash- and elemental contributions of the individual streams to the calculated Cuijk mixture in percentage values for the second series of fuel. 11 = relative concentrations of elements higher than the relative ash-contribution to the mix. 11 = relative concentrations of elements that are lower than the relative ash-contribution to the mix. 11 = the stream that contributes the largest fraction of the element to the mixture*

Fuel	Wood clippings 2 10%	Uprooted wood 2 6%	Thinning wood 2 10.5%	Sawdust 2 73.5%	Cuijk mix* 2 as analysed	Cuijk mix+ 2 calculated
Ash (at 550°C) as wt % of fuel	1.70	0.43	0.51	0.54	3.79	3,17
Ash (wt% in mix)	53.6	13.4	16.1	16.9	119.5	100
Elements in ash (wt% in mix)						
Cl	56.5	9.5	14.0	20.1	108.6	100
S	32.5	15.2	20.2	32.1	123.8	100
Si	81.3	10.3	7.1	1.3	164.7	100
Al	75.0	9.1	8.1	7.9	91.9	100
Na	59.5	9.1	16.2	15.3	92.4	100
K	33.7	12.6	21.0	32.7	116.9	100
Ca	27.7	17.5	23.9	30.9	108.7	100
Mg	31.0	13.6	19.3	36.1	108.0	100
P	32.9	17.5	24.5	25.1	129.0	100
Fe	50.1	15.7	12.0	22.1	179.0	100
Mn	16.0	4.7	5.1	74.1	82.6	100
Cr	59.1	9.9	6.9	24.1	197.0	100

* Cuijk-mixture consists of: 10% wood clippings, 6% uprooted trees, 10.5% thinning wood and 73.5% sawdust.

+ The calculated Cuijk mixture is based on the analyses of the individual streams in the mix multiplied by their percentage in the mix.

3.1.4 The difference between “winter” and “summer” wood fuels.

From the comparison of the first and second series of fuels from Cuijk, major differences become apparent, both for the individual streams as well as for the Cuijk mix. The first series are “winter” fuels and were harvested before the leaves came on the trees. The second series are summer fuels (except maybe for the sawdust) thought to be harvested in August/September. From the analyses in Appendix 1 and the contributions to the Cuijk mix as shown in Table 3.1 and 3.2, a number of important differences can be distinguished:

- The total ash content is much higher for the series 2 fuels, with exception of the sawdust. The ash content of wood clipping 2, uprooted trees 2 and thinning wood 2 are higher by factors of 6, 4 and 5 respectively. This has also implications for the contributions to the Cuijk mix. For the winter-fuels of series 1, 10% of wood clippings contributes 33% of the total ash, while for the wood clippings 2, the same mass percentage of wood contributes over 50% of the total ash in Cuijk mix 2. The opposite is the case for the sawdust. While sawdust 1 contributes more than 50% of the ash with 73.5% of the wood mass in the Cuijk mix 1, the sawdust only contributes 17% of the total ash with the same 73.5% of wood mass in the Cuijk mix 2.

- The higher ash content also results in higher concentrations of individual inorganic elements. However, not all elements increase with factors 4-6 for series 2 fuels compared to series 1. When for every (main) element a multiplication factor is calculated relating the concentrations in series 1 and series 2 wood fuels, the elements can be divided in two main groups. The elements Na, K, S, Ca, Mg, P and Mn are in the wood clippings 2, uprooted wood 2 and thinning wood 2 higher by factors 1.5-3 in comparison to the streams in series 1. While the elements Si en Al are higher by factors 5-6, in case of uprooted wood 2 even 50 times the Si content of uprooted wood 1. The division in two main groups with different multiplication factors gives a good indication for the enrichment origin of summer fuel compared to winter fuels. Based on knowledge of soil and inorganic plant composition, the following can be concluded. The main reason for the enormous increase in Si and Al can be contributed to attached sand (Si) and clay (Al and Si) in the summer fuels, leading also to a significant ash increase. The increase in total ash due to attached sand and clay is, based on the analyses, estimated to be 10% for the wood clippings 2, 2.6% for the uprooted trees 2, and approximately 1% for the thinning wood 2. This, however, does not explain the total increase in ash compared to the series 1 fuels. The fact that for plant physiology important elements, i.e. Na, K, S, Ca, Mg, Mn and P, in all cases increased by a factor of 1.5-3 compared to the wood series 1, indicates that the presence of leaves, transport fluids within the plants and general bio-activity leads to an increased ash percentage. In case of wood clippings 2, this is approximately 4.4%, for the uprooted wood 2, about 2.7% and for the thinning wood 2 approximately 3%.

The main conclusions from the comparison between winter and summer wood fuels is that for wood clippings, uprooted trees and thinning wood an increased ash content of 3-4% can be attributed to the inorganic elements required for physiologic plant processes and mainly present in the fast growing parts. Of the 3-4% ash increase an important part consists of problem causing elements in an FBC installation. The remainder of the ash increase can be attributed to higher amounts of attached sand and clay to the fuel. It leads to higher costs for ash disposal (due to higher ash quantities) but is not thought to lead to major technical problems within the installation.

The difference in problematic elements by a factor 1.5-3 can also be seen in the contributions to the Cuijk mix. In Table 3.1 it can be seen that sawdust with 73.5% of the wood mass contribute also the majority of most of the main inorganic elements (in red). In Table 3.2, the stream of 10 wt% wood clippings contributes the majority of the elements Cl, S, Na, K, Si and Al in the mix.

Note that the majority of numbers highlighted in red has shifted from the saw-dust 1 to the wood clippings 2 column.

The general believe that wood fuels are among the most unproblematic biomass fuels can be considered true for the winter fuels. However, in comparison with the other two fuels (olive stone pulp and cocoa beans) compared with the wood fuel in Section 3.1.3, the summer fuel could be easily equally problematic based on the general analyses. More specifically related to the agglomeration problem, the fuels analyses are calculated into agglomeration indicators in the next Section. It is aimed to come to an order in the fuel range used going from problematic to unproblematic fuels with respect to agglomeration using the agglomeration indicators.

3.2 Agglomeration indicators

In Section 2.3, the agglomeration indicators were introduced based on general experience. The agglomeration indicator I1, (Na + K)/ (2S + Cl) > 1, reflects the chance that an excess of alkali, over S and Cl, is likely to form alkali-silicates in the bed. The ratios of elements representing the agglomeration indicators are calculated here based on the available analyses in Appendix 1. The results are shown in Tables 3.3-3.5.

Table 3.3 *Chemical data of the first series of wood fuels and the calculated ratio of the agglomeration indicator I1*

Fuel/ Element concentration	K g/kg fuel	Na g/kg fuel	S g/kg fuel	Cl g/kg fuel	Indicator I1 (Na+ K) / (2S + Cl)
Cuijk mix 1	0.98	0.05	0.13	<0.33	>1.8
Wood clipping 1	2.30	0.32	0.29	0.14	3.6
Thinning wood 1	1.17	0.05	0.19	0.07	2.7
Uprooted trees 1	1.79	0.11	0.28	0.13	2.8
Sawdust 1	0.80	0.03	0.10	<0.40	>1.4

Table 3.4 *Chemical data of the second series of wood fuels and the calculated ratio of the agglomeration indicator I1*

Fuel/ Element concentration	K g/kg fuel	Na g/kg fuel	S g/kg fuel	Cl g/kg fuel	Indicator I1 (Na+ K) / (2S + Cl)
Cuijk mix 2	1.75	0.15	0.30	0.19	2.4
Wood clippings 2	5.05	0.95	0.79	0.99	2.3
Thinning wood2	3.00	0.25	0.47	0.23	2.8
Uprooted trees 2	3.16	0.24	0.61	0.28	2.3
Sawdust 2	0.98	0.03	0.11	0.05	3.7

Table 3.5 *Chemical data of the non-woody fuels, fuel mixtures of wood with other fuels and the calculated ratio of the indicator I1*

Fuel/ Element concentration	K g/kg fuel	Na g/kg fuel	S g/kg fuel	Cl g/kg fuel	Indicator I1 (Na+ K) / (2S + Cl)
Olive stone pulp	3.40	0.12	0.33	1.30	1.8
75% Cuijk mix 2 + 25% olive stone	2.16	0.14	0.23	0.59	2.2
Cocoa bean	4.17	0.11	3.10	1.00	0.6
90% Cuijk mix 1 + 10% cocoa bean	2.00	0.15	0.43	<0.40	>2.6

It can be concluded from Tables 3.3-3.5 that for all fuels, except for cocoa bean, the ratio is larger than one. Therefore, the first agglomeration indicator predicts a large chance that the excess alkali over the sum of chlorine and sulphur would stay in the bed and react to alkali-silicates. The formation of alkali-silicate is often observed to lead to sintering/de-fluidisation.

Although the indicator I1 predicts a large chance of alkali staying in the bed, the second agglomeration indicator, I2, provides more information on the chances that the formation of alkali-silicates will indeed result in agglomeration due to sintering of the coatings. As described in Section 2.3, the agglomeration indicator I2 describes the chance of the formation of a non-sticky outer coating based on the ratio of (K + Na+ Si) /(Ca +P + Mg). For a ratio smaller than 1, the refractory outer coating is likely to form and prevent the sintering of coatings. In Tables 3.6-3.8, the calculated ratios are given, based on the analyses in Appendix 1.

Table 3.6 *Chemical data of the first series of wood fuels and the calculated ratio of the agglomeration indicator I2. Data in blue are explained in the text.*

Fuel/ Element concentration	K g/kg fuel	Na g/kg fuel	Si g/kg fuel	Ca g/kg fuel	P g/kg fuel	Mg g/kg fuel	Indicator I2 (Na+K+Si) / (Ca+P+Mg)
Cuijk mix 1	0.98	0.05	0.13	1.58	0.15	0.22	0.6
Wood clipping 1	2.30	0.32	12.87	4.38	0.32	0.52	3.0
			(0.57)				(0.6)
Thinning wood 1	1.17	0.05	0.09	1.86	0.19	0.28	0.6
Uprooted trees 1	1.79	0.11	0.25	3.45	0.39	0.41	0.5
Sawdust 1	0.80	0.03	0.07	1.34	0.10	0.17	0.6

Table 3.7 *Chemical data of the second series of wood fuels and the calculated ratio of the agglomeration indicator I2. The data in red and blue will be explained in the text.*

Fuel/ Element concentration	K g/kg fuel	Na g/kg fuel	Si g/kg fuel	Ca g/kg fuel	P g/kg fuel	Mg g/kg fuel	Indicator I2 (Na+K+Si) / (Ca+P+Mg)
Cuijk mix 2	1.75	0.15	12.21	3.69	0.32	0.37	3.2
(Si=3*Cijkmix 1)			(0.39)				(0.5)
Wood clipping 2	5.05	0.95	60.24	9.41	0.82	1.05	5.9
(Si=3*wood cut 1)			(1.71)				(0.7)
Thinning wood 2	3.00	0.25	5.04	7.73	0.58	0.62	0.9
(Si= 3* thin wood1)			(0.27)				(0.4)
Uprooted trees	3.16	0.24	12.66	9.88	0.73	0.76	1.4
(Si=3* uproot 1)			(0.75)				(0.4)
Sawdust 2	0.98	0.03	0.13	1.43	0.09	0.17	0.7

Table 3.8 *Chemical data of the non-woody fuels, fuel mixtures of wood with other fuels and the calculated ratio of the agglomeration indicatorI2. Data in red will be explained below*

Fuel/ Element concentration	K g/kg fuel	Na g/kg fuel	Si g/kg fuel	Ca g/kg fuel	P g/kg fuel	Mg g/kg fuel	Indicator I2 (Na+K+Si) / (Ca+P+Mg)
Olive stone pulp	3.40	0.12	2.75	5.53	0.15	1.41	0.9
75%Cuijkmix 2 + 25% olive stone	2.16	0.14	9.45	4.15	0.28	0.63	2.3
(Si Cuijkmix=0.39)			(0.98)				(0.7)
Cocoa bean	4.17	0.11	0.15	1.70	0.72	2.06	1.0
90% Cuijk mix 1 + 10% cocoa bean	1.30	0.06	0.14	1.59	0.21	0.41	0.7

As can be concluded from the results in Tables 3.6-3.8, most of the ratios for the first series of wood are below 1, indicating that the formation of a refractory and protective outer coating can be expected and hence agglomeration is not expected based on the agglomeration indicators. Only the ratio for wood clippings gives a ratio above 1. However, this wood fuel is known to contain attached sand and this frustrates the fuel-Si value and thereby the total ratio value. The reason why it is important to distinguish between Si derived from within the biomass itself and Si from attached sand, is that the attached sand behaves itself (initially) relatively inert under the conditions within the FBC. This will be discussed in more detail in Section 4.

In an attempt to make a first distinction between fuel-derived Si and attached-sand derived Si, the Si value for the second series of wood fuels was taken to be 3 times the Si-value of the equivalent stream in the first series of wood fuels. This is based on the calculations that showed the differences between the summer and winter fuel, as described in Section 3.1.4. The differences were calculated to give higher element concentration for the summer fuels from higher plant physiology by a factor of 1.5-3 compared to the winter fuels, while the rest was attributed to a larger amount of attached sand. The factor 3 increase in elemental concentration is applied above for the Si-concentration and the resulting numbers are given in Tables 3.6-3.8 in red. It would result in ratios for the second wood series that by the new procedure become below 1, except for the wood clipping 2. The newly processed result of wood clippings 2, however, is based on wood clippings 1, which is already known to contain attached sand. Therefore, a second approximation is used to estimate the fuel-Si in the wood-clippings 1. The Si-value from the Cuijk mix 1 as analysed is taken, and subtracted from it, is the sum of the values (as analysed) for the contribution of sawdust, thinning wood and uprooted wood which leaves a value of 0.057 g for the contribution of 10% wood clippings per kg of fuel. Multiplying this value by 10, an estimate for the Si-value of 100% wood clippings is obtained, which is 0.57 g/kg

of fuel. For the wood clippings 2, again the assumption is made that it is three times the value of the wood clippings 1. These corrected Si-values are used in the corrected ratios indicated in blue in Table 3.7.

Based on the indicators I1 and I2, it is expected that all fuel (combinations) considered will lead to the formation of alkali-silicates in the bed (I1>1) Only cocoa bean as stand-alone fuel would be expected to be a fouling-fuel rather than a fuel leading to alkali-induced agglomeration (I1<1). Further, from the I2-ratios, all fuels are expected to form a refractory outer coating when using the corrected data for Si and the resulting ratios of I2 (in red and blue in Tables 3.6-3.8). As individual streams, both cocoa beans and olive stone pulp yield relatively large I2 ratios, with values of 0.99 and 0.88, respectively. The values for the individual streams in the Cuijk mixes and the Cuijk mixes themselves yield I2 values that stay below 0.7. Of the Cuijk fuels, wood-clippings 2 and wood clippings 1 give the highest values of I2.

Taking all data and difficulties into consideration, the observations under the SEM data must elucidate the formation of the refractory outer coating layer and its morphology as a continuous layer. For the future, it seems crucial to optimise the analysis methods so that a distinction between Si from attached sand and Si from the fuel can be made, which then allows the second agglomeration indicator to be used more effectively.

The interactions between the two agglomeration indicators I1 and I2 are neglected here for simplicity. The assumption is made that they apply in consecutive order, first I1 and *IF* the ratio is larger than 1, then I2 is considered. Although some interaction of e.g. K with Si in the bed material is likely to occur, no matter how high the Cl concentration is, it is assumed that the gas phase reactions resulting in alkali-halides and –sulphates are much faster than the reactions in the bed and thereby that the gas phase reactions dominate the first segregation of alkalis between gas phase and bed material.

The assumption made with regard to indicator I2, is that as a first approximation the total fuel content of the alkalis is used. The consecutive use of I1 and I2 would suggest that the concentration of alkalis equivalent to the total concentration of (Cl + 2S) would be subtracted from the total concentration in the fuel before the ratio I2 would be calculated. The subtracted concentration would represent the fraction being expelled to the gas phase and not available for alkali-silicate formation in the bed. However, because it is unknown if the outer coating formation requires the same mass of (Ca+P+Mg) as the mass of (K+Na+Si) present, to counteract the stickiness of the inner coating, in other words, if the best criterion would be an I2 ratio of 1, it seems inappropriate to go into further detail at the moment. In case the appropriate value for I2 can be established in the future, then the concentration of the alkalis can be further refined by the above-described subtraction of gas-phase alkalis.

A third assumption regarding the values of I1 and I2 is made for mixtures of e.g. cocoa bean or olive stone pulp with wood. Assumed is that the ash components of both fuels in the mix are thoroughly mixed on an elemental scale and therefore elements of both fuels can be added up in the calculation of I1 and I2. Especially for I2 the results in practice could be substantially different if fuel particles slowly release elements in the bed and local circumstances are dominated by ash particles from individual fuels.

3.3 Results of the WOB-tests

All WOB-tests were carried out successfully and the experimental matrix is shown in Table 1. The series 1 test run for a standard period of 8 hours. Series 2 and 3 did run as long as the prepared fuel was available. Only tests 12 and 13 were stopped early because of agglomeration.

Table 3.9 *Combination of fuel and bed materials used in the WOB experiments, duration of the tests and timing of sampling. Average coating thickness of coating layers in the samples is indicated*

Test/date	Fuel(s)/ bed material	Duration of the test (h)	Bed material sample time (total)	Average coating thickness (SEM-analyses).
Series 1: test 1/ 1 July 2002	Wood clippings 1/ Un-used Cuijk sand	8	-4h -8h	- n.d. -average 2.5-3 μm++
Series 1: test 2/ 2 July 2002	Uprooted trees 1/ Un-used Cuijk sand	8	-4h -8h	- n.d. -2-10 μm ++
Series 1: test 3/ 3 July 2002	Thinning wood 1/ Un-used Cuijk sand	8	-4h -8h	- n.d. -average 3 μm ++
Series 1: test 4/ 4 July 2002	Sawdust 1/ Un-used Cuijk sand	8	-4h -8h	- n.d. -average 2 μm
Series 1: test 5/ 5 July 2002	Cuijk mix 1*/ Un-used Cuijk sand	8	-4h -8h	- n.d. -average 2 μm ++
Series 1: test 6/ 5 and 6 November 2002	Cuijk mix 1* + 15% cocoa bean/ 885g bed material from test 5 + 175g un-used Cuijk sand	13.5	-13h (5+8) -21.5h (13.5+8)	-average 3 μm -average 6 μm
Series 2: test7/ 20 and 21 January 2003	Wood clippings 2/ 755g bed material from test 1 + 305g un-used Cuijk sand	11.5	-14.5h (6.5 h+8) -19.5h (11.5+8)	-average 5 μm -average 11 μm
Series 2: test8/ 27 and 28 January 2003	Uprooted trees 2/ 759g bed from test 2 + 301g un-used Cuijk sand	15	-17h (8+9) -23h (8+15)	-n.d. -average 8.5 μm
Series 2: test9/ 29 and 30 January 2003	Thinning wood 2/ 811g bed from test 3 + 249g un-used Cuijk sand	11	-14h (6+8) -19h (11+8)	-n.d. -average 13 μm
Series 2: test10/ 22,23 and 24 January 2003	Sawdust 2/ 899g bed from test 4 and 161g un-used Cuijk sand	16.5	-18.5h (10.5+8) -24.5h (16.5+8)	-average 4.5 μm -average 5 μm
Series 2: test 11/ 30 and 31 January 2003	Cuijk-mix* 2/ New olivine material as bed material	11.5	-5h -11.5h	-average 1 μm -average 3.5 μm
Series 3: test 12/ 20 December 2002	75 wt% Cuijk-mix 2* + 25 wt% olive stone. /un-used Cuijk sand	6 h/, stopped due to agglome-ration	-6h	-average 6 μm *Thick reaction zones (inner coating).*
Series 3: test 13/ 26 February 2003	75 wt% Cuijk-mix2 * + 25 wt% olive stones / 712g bed from test 12 + 348g un-used Cuijk sand	2.5 h test, stopped due to agglome-ration	-8.5h (2.5 +6)	*Sample seems unchanged from sample test 12*
Series 3: test 14/ 6 March 2003 (same test conditions as test 12 but with lower fluidisation velocity 70 l/min instead of 95 l/min)	75 wt% Cuijk-mix2* + 25 wt% olive stones./ un-used Cuijk sand	5.5h	never really stable fluidisation -5.5 h sample	Not studied because of uncertain conditions

* Cuijk-mix consists of: 10% wood clippings, 6% uprooted trees, 10.5% thinning wood en 73.5% sawdust.
++ the average coating thickness is unevenly distributed over the grain. N.d. is “not determined”.

3.4 SEM observations

Scanning electron microscopy data, both morphological and chemical data, form the key element to coating development modelling. Because the dataset per sample is extremely large and complicated, a more extensive description is given for only 2 representative fuels, namely for wood clippings and for the uprooted trees fuels, and even for these fuels chemical data have been averaged. For the remaining bed material/fuel combinations a much shorter description is given and referencing to the first two sample descriptions is used as much as possible. The thickness of the average coating layers is given in Table 3.9 in order to provide an overview of the experimental conditions in combination with the resultant coatings.

3.4.1 Wood clippings samples

Two tests are indicated in Table 3.9, that were performed using wood clippings as fuel, i.e. test 1 and test 7. The first test was performed with the "winter" fuel while test 7 was a longer duration experiment with the "summer fuel". The latter test was performed with the remaining bed material from test 1. However, due to material loss during cleaning of the installation, approximately 1/3 of the bed was new/un-used bed material. The samples available were taken after 8, 14.5 and 19.5 hours of total test duration. It must be kept in mind then, that 1/3 of these bed material grains in the last 2 samples were only used for 6.5 and 11.5 hours. Because no distinction can be made between the grains that did run the full test run and the grains that were introduced only in the last test an average coating thickness shall be calculated. Because the feeding rate during the test was known as well as the ash content of the fuel, it could be calculated which fraction of the ash ended up in the coating layers.

The following results in coating thickness were obtained:

- Coating thickness after 8 hours: average 2.5-3 micron, which is equivalent to 12.5% of the ash input ("winter fuel") and an absolute amount of 2.3 g/hours in coating build-up.
- Coating thickness after 14.5 hours: average 5 micron, which is 2.75% of the ash input from the last 6 hours. In this calculations it was assumed that 2/3 of the grains had coatings that grew from 3 to 5 micron, while 1/3 of the grains had coatings that grew from zero to 5 microns ("summer fuel"). In absolute amount, 2.9 g/h was used in coating build-up, with the same fuel-feeding rate.
- Coating thickness after 19.5 hours: average 11 micron, which is. 7.3% of the ash input from the last 5 hours. In absolute amount 7.85 g/h was stored in coating build-up.

From the small difference in absolute values of material being stored in coating build-up, it can be concluded that the large increase in ash between winter and summer fuel, only partly results in the faster growth of coating layers. Additional information comes from the increase in bed material weight during this test. From the total bed-weight increase only 31% became stored as coatings. The remainder of the bed weight increase is likely to be attributable to attached sand on the fuel.

In terms of coating morphology:

- After 8 hours the coating consisted mostly of a single layer, although some spots of K-silicate reaction zones were present. The coating layer was thin but nearly continuous. The reaction spots were thick if present. From morphological data it can be established that the reaction zones are at least partly due to diffusion/dissolution of K into the quartz grains.
- In the samples taken after 14.5 and 19.5 hours the reaction layer of K-silicate becomes more continuous in coverage but still varies largely in thickness (see Figure 3.1). The outer coating layer is mostly a continuous layer. In the last sample, occasionally the appearance of a middle layer can be found. This middle layer seems to develop with time by segregation from the inner and outer coating.

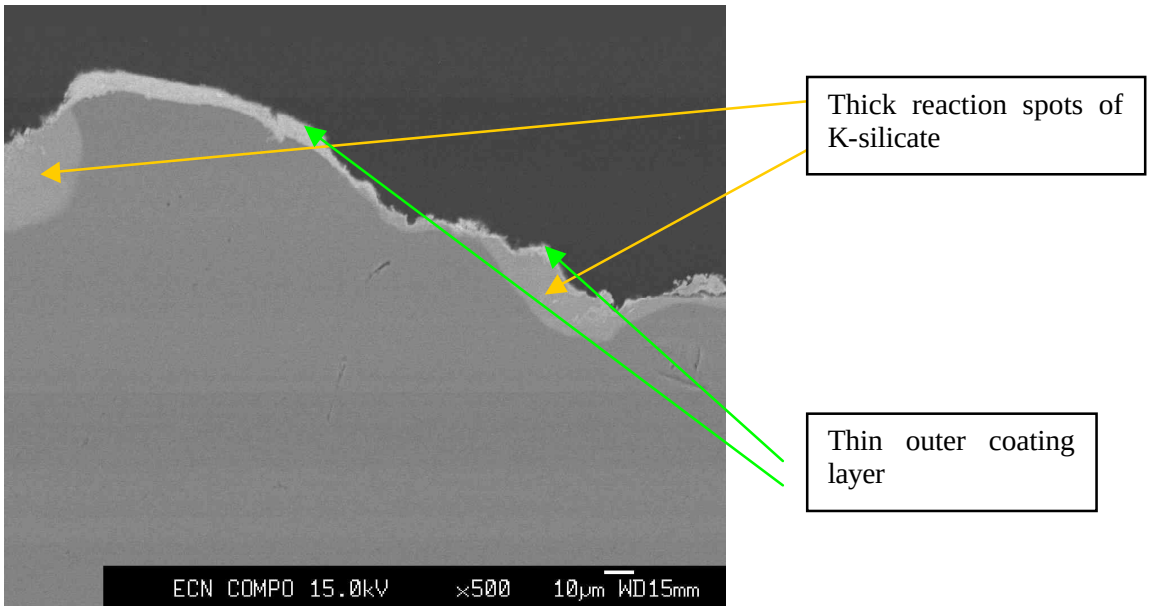

Figure 3.1 *SEM micrograph showing a section of a bed material grain after 14.5 hours of use in the WOB while combustion Wood clippings. Indicated are the thick reaction spots and the lighter coloured outer layer coating on the quartz grain*

The average coating chemical compositions are given in Tables 3.10 and 3.11. Table 3.10 shows the chemical composition of the reaction (inner) layer with time and Table 3.11 the average composition of the outer layer with time.

Table 3.10 *Chemical composition of the reaction layer with time for wood clippings as fuel on SiO_2 bed material. For ease of comparison, the main elements are given in round numbers*

Element (wt%) in the reaction layer	After 8 hours	After 14.5 hours	After 19.5 hours
Si	35 ± *4*	36 ± *3*	33 ± *4*
K	8 ± *4*	9 ± 1	12 ± *2*
Ca	3 ± *2*	4 ± *1*	5 ± *2*
Na	2 ± *1*	2 ± *1*	3 ± *1*
P	0.3 ± 0.2	1.0 ± 0.5	1.0 ± 0.5
Mg	0.5 ± 0.3	1.0 ± 0.6	0.8 ± 0.5
Fe	1.1 ± 0.2	2 ± 1	3 ± 3
S	0.0	0.0	0.0

Table 3.11 *Chemical composition of the outside coating layer with time for wood clippings as fuel on SiO_2 bed material (no distinction is made between middle and outer layer).*

Element (wt%) in de coating	After 8 hours	After 14.5 hours	After 19.5 hours
Si	7.5 ± 2.5	5.9± 0.7	6.0 ± 2.0
K	0.7 ± 0.3	1.8 ± 0.7	5 ± 3
Ca	29.0 ± 2.0	29.0 ± 2.0	27 ± 4
Na	0.5 ± 0.2	1.2 ± 0.6	1.4 ± 0.3
P	3.7 ± 1.5	5.5 ± 0.5	4 ± 1
Mg	5.2 ± 1.5	4.4 ± 1.5	4 ± 2
Fe	5.0 ± 2.0	5.8 ± 1.5	6 ± 2
S	0.5 ± 0.3	2.1 ± 0.7	3.3 ± 1.5

From the Tables 3.10 and 3.11, it can be seen that with time Si in the reaction layer is constant while K increases from 8 to 12 wt%, Ca slowly increase to 5 wt%. Other elements give only minor to negligible contributions. The outer coating layer also shows a constant Si content of roughly 6 wt%, Ca is also constant with ~28 wt% and Mg and P contribute roughly 4 wt% each, Fe 5 wt%. The outer coating chemistry is remarkably constant with time. Only K and S slowly increase with time. A possible explanation is that the K-diffusion to the SiO_2 grain becomes slower once the reaction layer becomes thicker. K-input might become faster than the diffusion and the resultant is some K in the outer layer. Once K is present in the outer coating, the reaction with S from the gas phase can be expected.

At the end of the total test period, the coating growth velocity is not diminishing yet, but no signs of agglomeration were found. Apparently, enough of the refractory outer coating has developed to prevent sintering due to the K-silicate reaction layer. The amount of K or K_2SO_4 in the outer layer is not sufficiently high to result in sticky behaviour.

3.4.2 Uprooted trees samples

The two tests performed with uprooted trees wood, as indicated in Table 3.9 are Test 2 and Test 8. The first was performed with the “winter fuel” the second was a longer duration test and was performed with the “summer fuel”. The latter test was performed with the remaining bed material from Test 2. However, due to loss during cleaning of the installation, approximately 1/3 of the bed was new/un-used bed material.

The following results in coating thickness were obtained:

- Coating thickness after 8 hours: average 3 micron, which is equivalent to 20% of the ash input (“winter fuel”) and an absolute amount of 2.3 g/hours in coating build-up.
- Coating thickness after 16 hours: average 5 micron, which is 3.7% of the ash input from the last 8 hours. In this calculations it was assumed that 2/3 of the grains had coatings that grew from 3 to 5 micron, while 1/3 of the grains had coatings that grew from zero to 5 microns (“summer fuel”). In absolute amount, 2.39 g/h was used in coating build-up.
- Coating thickness after 22 hours: average 8.5 micron, which is. 4.6% of the ash input from the last 5 hours. In absolute amount 3.9 g/h was stores in coating build-up.

From the small difference in absolute values of material being stored in coating build-up, it can be concluded that the large increase in ash between winter and summer fuel only partly results in the faster growth of coating layers.

In terms of coating morphology:

- After 8 hours the coating consisted mostly of a single layer, although some spots of reaction zones to K-silicate were present. The coating layer was less evenly distributed as for the wood clipping samples. The reaction spots were thick if present. From morphological data it can be established that the reaction zones are at least partly due to diffusion/dissolution of K in the quartz grains.
- Two types of initial coating can be found, an initial coating with K and one without K (no reaction layer)
- In the samples taken after 16 and 22 hours the two types of different initial coatings develop differently with time. The initial layer without K develops in an inner coating, which is a Ca-silicate, in which Si is the main component and an outer coating, which is also mainly Ca-silicate in which Ca is the main component. The other type of initial coating develops almost identical to the situation described for wood clippings, including the development of a middle layer.

The average coating composition with time is given in Tables 3.12 and 3.13. The tables are now organised differently. Table 3.12 slows the chemical development of one of the types of initial coating (Type A), which develops with time in two layers of coating with composition $X(/A)_{inner}$ and X_{outer}. The chemical composition of the other (wood clippings) type initial coating (Type B) is given in Table 3.13, together with its chemical development in $Y(/B)_{inner}$, Y_{middle} and Y_{outer} coating.

Table 3.12 *Chemical average composition of the coatings for uprooted trees as fuel and SiO_2 as bed material. The indications for the 16 h sample is X/A because it is in many aspects intermediate between the 8 and 22 hours samples*

Element (wt%)	After 8 hours Type coating A	After 16 h Type coating X/A_{inner}	After 16 h Type coating X/A_{outer}	after 22 h Type coating X_{inner}	After 22 h Type coating X_{outer}
Si	7.0	10.0	3.0	14.0	3.4
K	0.5	0.7	10.0	0.4	8.0
Ca	32.0	40.0	31.0	40.5	28.0
Na	0.5	0.5	0.9	0.4	1.3
P	5.8	5.2	7.9	2.9	5.0
Mg	6.4	3.1	7.8	0.9	4.6
Fe	2.5	2.5	2.8	0.6	5.9
S	1.4	0.9	3.8	0.4	4.1

Table 3.13 C*hemical composition of the coatings for uprooted trees as fuel and SiO_2 as bed material. The indications for the 16 h sample is Y/B because it is in many aspects intermediate between the 8 and 22 hours samples*

Element (wt%)	After 8 h Type coating B	After 16h Type coating Y/B_{binnen}	After 16h Type coating Y/B_{midden}	After 16 h Type coating Y/B_{buiten}	After 22h Type coating Y_{binnen}	After 22h Type coating Y_{midden}	After 22h Type coating Y_{buiten}
Si	31.0	36.6	26.2	10.3	34.5	17.8	3.0
K	0.2	9.7	0.4	2.6	10.2	0.4	7.0
Ca	11.0	8.3	38.3	39.5	5.3	44.0	29.0
Na	0.2	1.4	0.3	0.7	1.8	0.4	1.3
P	1.9	0.2	0.4	3.9	0.3	1.0	6.0
Mg	1.3	1.7	0.0	2.1	0.5	0.1	6.7
Fe	0.8	0.4	0.3	2.6	1.3	0.2	3.2
S	0.3	0.0	0.2	0.9	0.0	0.0	4.2

From the Tables 3.12 and 3.13 it can be concluded that the build-up of the coatings follows the general description:
Type A$\rightarrow$ $X(/A)_{inner} + X_{outer}$
Type B$\rightarrow$ $Y(/B)_{inner} + Y_{middle +} Y_{outer}$

For Type A, the inner coating layer has a ratio Si:Ca as 1:3-4 while the outer coating develops to a ratio Si:Ca as 1:10. Remarkable is further the virtual absence of K in the inner layer and the increase of K to 8-10% in the outer layer. Together with the K appears again the S in the outer layer and close to the ratio that suggests the formation of K_2SO_4. The initial low content of K seems to promote the formation of a Ca-silicate inner coating, which with time stays a Ca-silicate and K stays in the outer layer.

For Type B, the initial K content in the 1 layer coating is also low, but similar to the observations for wood clipping samples, some larger spots of K-silicate are present occasionally. Type B develops in an inner coating, which contains 10 wt% K , 34 wt% Si and 5 wt% Ca. This is equivalent to the wood clippings samples. The middle coatings is a Ca-silicate and the outer coating is high in Ca and the refractory elements. All very similar to the wood clippings samples. The contents of K and S follows also the same pattern. Only at a later stage some K becomes present in the outer layer and with K also S appears.

Note that for the 22 hours sample the concentration of K ad S in the outer coatings is the same for type X and Y. In fact the total composition of the outer coatings of the two types has become very similar.

3.4.3 The SEM samples for the thinning wood samples, the sawdust samples and the Cuijk mix samples

The samples of the thinning wood fuel are intermediate between the wood clippings and the uprooted trees samples. Both types of coating development are present. However, the development of:

Type B$\rightarrow$ $Y(/B)_{inner} + Y_{middle +} Y_{outer}$

is dominant. The chemistry of the coating layers is (within the error margins) identical to that same type of coating in both the wood clippings and the uprooted trees samples. This means that the inner layer has a composition of Si = 33 wt%, K = 11 wt% and Ca = 5 wt%, the middle layer

is a Ca-silicate with Ca = 41-43 wt% and Si = 14-18 wt%, while the outer coating layer is Ca = 33-35 wt%, P = 5 wt%, Mg = 6-8 wt% and Si = 6 wt%. The average coating thickness after 19 h experiment is 13 micron.

The samples of the sawdust fuel, again follows the same pattern of coating build-up. Both initial types are present again, but similar to the thinning wood samples, the type of

Type B→ $Y(/B)_{inner}$ + Y_{middle} + Y_{outer}

Is dominant. The chemistry is, within the error margins, once again identical to all the compositions described above.
Due to the very low ash content, the total coating build-up after 24.5 hours of experimentation is only 5 micron. However, although the total ash content is lower by a factor of 3-10 compared to the other individual Cuijk streams, the coating thickness is only thinner by a factor 0.5-2, which confirms again that the ash content is only partially represented in the velocity of coating build-up.

The sample of the Cuijk mix after 8 hours shows a coating thickness of 2 micron with a composition similar to the previous samples. Reaction spots of K-silicate are present as well as a single coating layer, which is more or less continuous. The bed material from this test was used for the test with 85% Cuijk mix and 15% cocoa bean, which will be described below.

3.4.4 SEM samples from the Cuijk mix with non-woody fuel mixtures

The sample of the test using the Cuijk wood mix as fuel with 25% olive stone pulp was obtained after 8.5 hours when the bed agglomerated. The total sample fell apart after cooling of the installation, so unfortunately no real agglomerates could be studied, but this seems to be a sample that can be considered representative for the onset of agglomeration. The total coating thickness was much larger than in the case of all the other only-wood-derived samples. An average coating thickness of 6 micron was obtained within the 8.5 hours and many thick spots of K-silicate reactions were present up to 70 micron in thickness.

The chemistry of the reaction spots were the same as for the wood-only reaction layer, i.e. Si = 33 wt%, K = 11 wt% and Ca = 4 wt%; in addition some Na was present up to 4 wt%. The outer layer consisted mainly of Ca-silicate, but varies now between ratios close to Ca: Si = 1:1 and Ca: Si = 3:1. Often an intermediate layer of Ca-silicate was already present. The agglomeration seems to be attributable to the thick spots of K-silicate, which are thicker and more abundant than in the wood-only samples.

The fact that the second agglomeration indicator suggests that sufficiently refractory elements should be present to form a non-sticky outer layer (when using the Cuijk 2 value corrected for attached sand) seems not in line with the observations. However, the ratio of K/Si is so high (red Si value in Table 4), that a very low melting product of the olive stone fuel could easily result in agglomeration due to large K-silicate spots, before the refractory outer layer could come into play. It is proposed that a third agglomeration indicator should be introduced, i.e. the ratio K/Si > 1 that would result in a type of agglomeration that is probably more closely related to melt-induced sintering (type 2 in Figure 2) than due to the sintering of coatings.

The sample of the Cuijk mix as fuel combined with 15% cocoa bean shows a coating build-up over time that is very similar to the wood-only type of fuels as described above. Both the coatings with only Ca-silicate as the reaction layer and coatings with K-silicate as reaction layer are present (type X and Y) and roughly in equal amounts. Further no distinction can be found between the samples with the cocoa bean and the samples from wood only.

3.4.5 SEM samples from the Cuijk mix fuel with Olivine as bed material

In test 11 (see Table 3.9) another type of bed material was used in combination with the Cuijk mix fuel. This bed material is Olivine, like quartz a natural material and its chemical composition is $(Mg, Fe)_2SiO_4$. The Mg and Fe within brackets indicate that the Mg^{2+} and Fe^{2+} are interchangeable on the same crystal sites and therefore the pure Fe_2SiO_4 and Mg_2SiO_4 form a perfect solid solution, i.e. any fraction division between Fe and Mg is possible. The olivine used in this test is Fo_{93}, which indicates the presence of 7 wt% Fe and 93 wt% Mg in the crystals.

Where every type of wood and even the wood plus other fuel mixtures resulted in remarkable similar coatings on quartz sand, this is the only test in which the coating build-up is totally different. Two coating layers develop in the relatively short test duration (11.5 hours). The inner reaction layer is a Ca-Mg-silicate, which in the first sample after 5 hours is very close to the formula for Montecelite (Ca:Mg: Si = 1:1:1). However in the later sample the composition of the reaction layer more often deviates from this composition towards higher Ca-values and is on average the composition becomes: Si = 10-15 wt%, Ca = 18-22 wt% and Mg = 10-16 wt%. Absolutely no K is present in the reaction layer in any of the observed coatings. K, and S are present in the outer coating layer. In general, the outer coating composition is more variable as in the case of the coatings on quartz. Observed to be present in the outer coatings most of the time are: Ca, Si, P, Mg, K, S and Fe. The coating thickness was on average about 1 micron after 5 hours and roughly 3.5 micron after 11.5 hours.

The experiment is too short to make suggestions for the behaviour in the long term and its potential to agglomerate. However, the outer coating is in general refractory of composition and therefore its potential to agglomerate likely depends on the increase with time of the K and S, which is an unknown factor at present.

3.5 Comparison between lab-scale and commercial-scale Cuijk samples

The usefulness of the lab-scale derived samples and the obtained physical/chemical models for practical applications depends largely on the similarity between the lab-scale samples and the samples from the commercial-scale installation at Cuijk. In order to investigate the degree of similarity, the coatings on bed materials from Cuijk were studied in detail.

Three types of samples were available from Cuijk to be compared with the samples obtained in the WOB. These are:

1. A sample taken 6 days after start-up following an extensive planned maintenance stop, with a fully new bed and cleaned installation.
2. A sample taken during continuous operation, that regarding the sample timing was roughly halfway between the last and next scheduled stop and not in any way associated with agglomeration during operation, before or shortly after sampling. In other words, a sample associated with un-problematic operation.
3. Three samples taken for the " EU-project BIFIC"[8], in which cocoa beans were used as secondary fuel to the ordinary Cuijk wood mix. The samples are from the tests with 5%, 10% and 15% cocoa beans, respectively.

Two major differences must be taken into account between the full-scale Cuijk plant and the laboratory-scale WOB (other than scale):

1. In Cuijk the fuel feeding takes place above the bed, while in the WOB, the feeding of the fuel is in-bed. This might make a difference in the degree that alkali and S are maintained in the bed, because the contact time of the alkali and S with the bed material is different.

2. In the Cuijk installation a schedule of bed material renewal is running which, at the time these samples were taken, replaced about 1/5 of the total bed in 24 hours. A schedule of discharging and replacing bed material did run on a 4-6 hours basis. From statistics it can be easily shown that it takes 20 days to have 90% of all original sand grains replaced. In the WOB, no bed material was replaced during the tests. Especially for late phenomena in coating build-up, such as the K and S appearance in the outer coating, both differences could be of importance.

The aim of the comparison between the WOB and the Cuijk samples is to get on the one hand a "feel" for how well the coating build-up of the WOB compares with the coating build-up in Cuijk, especially because in case of a close resembling the WOB could be used as a predictive tool for testing future fuel-mixtures and fuel/bed material combinations. On the other hand, if the coating build-up is similar, the Cuijk samples can be used for extrapolation of the coating behaviour with time, because all the Cuijk samples (despite the replacement of bed material) represents coatings existing on average for much longer times than obtained those in the WOB.

3.5.1 The 6 day sample

The sample taken after 6 days is from using the ordinary Cuijk wood mix and the ordinary quartz bed material. Within the 6 days of operation, sand replacement took place, although in the first few days at a lower frequency. Figure 3.2 shows a section of a sand grain with a typical coating morphology and chemistry. An inner and outer coating layer can be clearly distinguished.

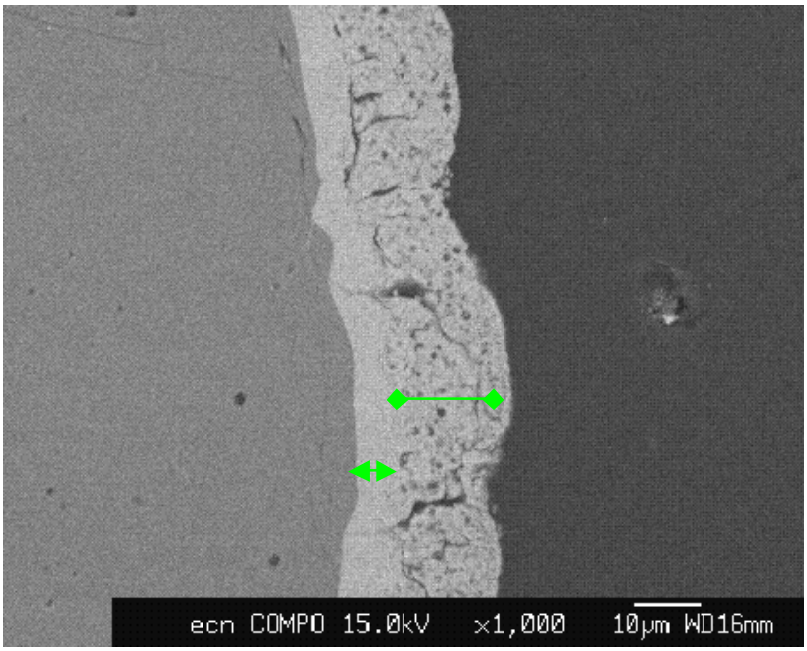

Figure 3.2 *SEM micrograph showing a section through a sand grain with coating. The green bars indicate the inner and outer coating that are both morphologically and chemically different*

The average coating thickness is 14.5 microns. However, the spread in coating thickness is much wider as for the WOB samples due to the bed material replacement. Coating thickness up to 60 micron were observed occasionally. The coating thickness range of 20-24 microns was however, best represented.

The most remarkable observation, however, comes from measuring the chemistry. The dense inner coating layer is either a K-silicate or a Ca-silicate. For the K-silicate the K-concentration

is on average 11 wt%, Si = 31-34 wt% and Ca = 5-8 wt%. This is the exact composition from the K-Silicate reaction zones observed in the WOB-samples. In the case the reaction coating is Ca-silicate, the ratios of Si:Ca vary, but other elements are nearly absent and hence this coating is also comparable to the Ca-silicate reaction layers in the WOB samples.
The outer coating contains Ca as the main element, with a content of 30-36 wt%, further a 6-8 wt% Si, 6 wt% Mg and approximately 5 wt% P. This coating also is very similar to the refractory coating observed in the WOB samples. More importantly it shows that over time a beautiful homogeneous and continuous layer of this refractory coating is build-up and maintained. It is the most important asset in this fuel/bed material combination that will prevent agglomeration.

The only main difference observed in the coating chemistry is that no K or S was observed to appear with time in the outer coating.

3.5.2 The Cuijk sample of continuous operation

The sample taken during continuous operation is from using the ordinary Cuijk wood mix and the ordinary quartz bed material. Sand replacement took place with a frequency of every 4 hours. After the longer period of regular discharge and replacement of bed material, a reproducible grain coating thickness must have established.

The starting bed material grain size is between 0.8-1.2 mm. The observed spread in coating thickness for particles > 1.2 mm is 20-50 micron, which is clearly thicker than for the sample taken after 6 days. A roughly determined average coating thickness for the continuous operation sample is 35 micron. For the grain sizes < 1.2 mm, a similar spread in coating thickness can be observed as for the 6 days sample. The smaller grain sizes also contain relatively many grains with thin coatings. Up to 3-4 micron, the coating layer consists often only of 1 layer, however, nearly all thicker coatings consist of an inner and outer coating. The chemistry of the inner and outer coating is the same as for the 6 days Cuijk sample, indicating that with longer residence times in the bed no further changes other than growth of the coating thickness occur. Based on the statistical residence time when taking the replacement schedule into account, the grains of the 6 days sample have an average residence time of 4.0 days, while for continuous operation (> 20 days), the grains have an average residence time of 5.8 days.

The observation that the average coating thickness of 35 micron does not lead to sintering of the coatings can be fully attributed to the refractory outer coating. With the bed renewal rates applied at the times of these samples, an adequate and sufficiently high frequency scheme of renewal rates was in place.

Samples studied from earlier days of the Cuijk plant showed that agglomerates could be attributed to a K-(Ca)-silicate “glueing” phase in which other phases and element concentrations of e.g. Ca-P and Mg were not involved. The thickness of the glueing patches and necks between two sand grains suggests that 35-40 micron thick coatings are involved in agglomeration. This would mean that the outer coating would be in some way eroded, corroded or chemically dissolved. No indications are available at the moment on the link between the inner coating of most bed material grains and the occurrence of agglomeration/sintering, except for the fact that the chemistry is very similar.

3.5.3 Cuijk samples from tests with a mixture of Cuijk wood mix and cocoa bean

Three samples were studied from tests in Cuijk using 5, 10 and 15% fuel on energy base from cocoa beans in combination with the regular Cuijk wood mix. In total, the cocoa bean test run for 1 week at the end of a long period of stable operation just before a planned maintenance stop. The bed material renewal rates were at as frequent as for the other samples.

The average coating thickness obtained for the samples was 21 micron for the 5% cocoa bean sample, 23 micron for the 10% cocoa bean test and 27 micron for the 15% cocoa bean test. In all three samples, coatings were split in 2 or 3 concentric layers. The inner reaction zone was in all cases now a K(Ca)-silicate, with exactly the same composition as for the wood-only fuels, namely 10-12 wt% K, 32-34 wt% Si and 4-6 wt% Ca. The middle layer when present was again a fairly pure Ca-silicate. At some places, even crystals had developed in the middle layer growing into the reaction zone with a Si: Ca ratio of 2:1, while the middle layer itself was of a Si:Ca ratio of 1:2. This seems to be a further advanced stage in time of the continuously developing coating layers.

The outer layer, finally, was again the known Ca-dominated refractory layer with additional element such as P and Mg. No K or S was present in the outer layer. Except for the latter detail, the Cuijk mix/cocoa bean samples therefore perfectly fit the description of:
Type B→ $Y(/B)_{inner} + Y_{middle +} Y_{outer}$

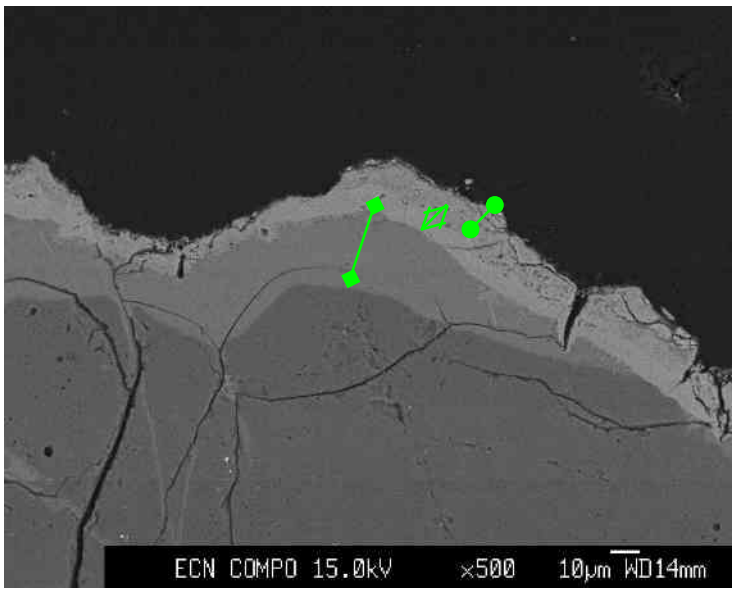

Figure 3.3 *SEM micrograph showing a section of a quartz grain from Cuijk taken after the test with 10% cocoa beans. The green bars indicate the three layers of coating*

3.6 Models

First of all, it must be emphasized that the chemistry of the coatings as observed from the lab-scale WOB are in nearly every aspect identical to those in Cuijk, to a degree that the chemistry variation within samples is larger than between samples. This is a much better fit then hoped for! The only difference is the late appearance of K and S in the WOB-samples outer coating, while this is not found in the Cuijk samples. This is thought to be due to the difference between no renewal in the WOB and the sand replacement in Cuijk. Although still speculative, the best explanation seems to be that when constantly fresh SiO_2 surface is supplied, the K will find its way preferably/more quickly to the newly formed reaction zones than on existing grains in which diffusion to the reaction zone has become too slow to keep up with the K-input.

In general coating thicknesses in the Cuijk samples are much larger than the thicknesses observed in the WOB, but this can be directly linked to the residence time in the bed. A first rough average gives a coating thickness of 2 micron after 8 hours and 10-12 micron after 24 hours and when the Cuijk data can be used as an extrapolation in time, then with a full bed load replaced in about 5 days the stable coating thickness goes to 20-35 micron for the fuel/bed material combinations investigated.

In fact, all the samples using quartz as bed material follow the same coating chemistry build-up with time. This was also an unexpected finding. In term of thickness some variation exists, which correlates with the ash content of the fuel, but not linearly. The increase in coating thickness is less than the absolute increase in ash.

Considering the build-up of coatings, 2 types were observed, and most samples contained both, although in varying fractions.
The two types were earlier indicated as:

Type A$\rightarrow$ $X(/A)_{inner} + X_{outer}$
Type B$\rightarrow$ $Y(/B)_{inner} + Y_{middle +} Y_{outer}$

Schematically the resultant coatings are illustrated in Figure 3.4.

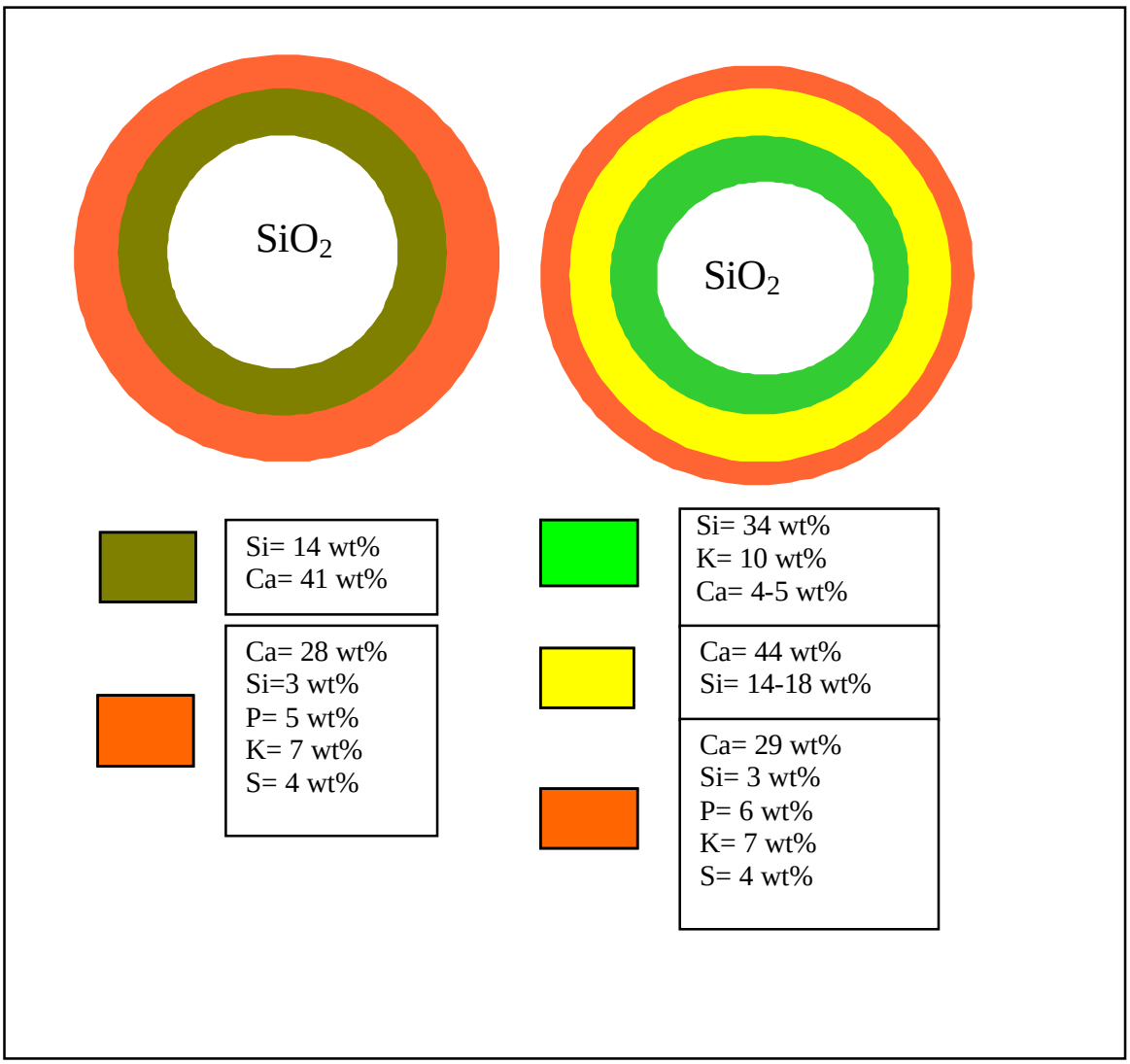

Figure 3.4 *Schematic models showing the two final types of coatings that develop on quartz bed material grains. On the left side, the model that represents the initial K-absent situation and the inner coating develops as a Ca-silicate. On the right-hand side, the model that represents the initial build-up of a K-rich inner coating.*

In Figure 3.4, the composition given is for the samples of the WOB. However, without the K and S in the outer coating the normalised analyses is equivalent to those observed for the Cuijk samples. As can be seen, in the final coating configuration, the outer layers are nearly equal in composition. Also the reaction zone of the left grain has become chemically equivalent to the middle layer of the right hand model, so that in fact the K-silicate reaction layer remains the only real difference between the two types that developed along different routes. The formation of the two-layer coating seems to depend on the absence of K. When no K is available, the most preferable reaction is to a Ca-silicate. Ca is more abundant in the fuel and from the K available a large fraction is likely to leave the installation as chlorides and sulphates. The predominance of a Ca-silicate reaction layer seems therefore most likely. Maybe the very K-rich fuel fragments can lead locally to different circumstances. Based on the observations in this study, the model as illustrated in Figure 3.5 is proposed for the 3-layer coating with a K-silicate reaction layer.

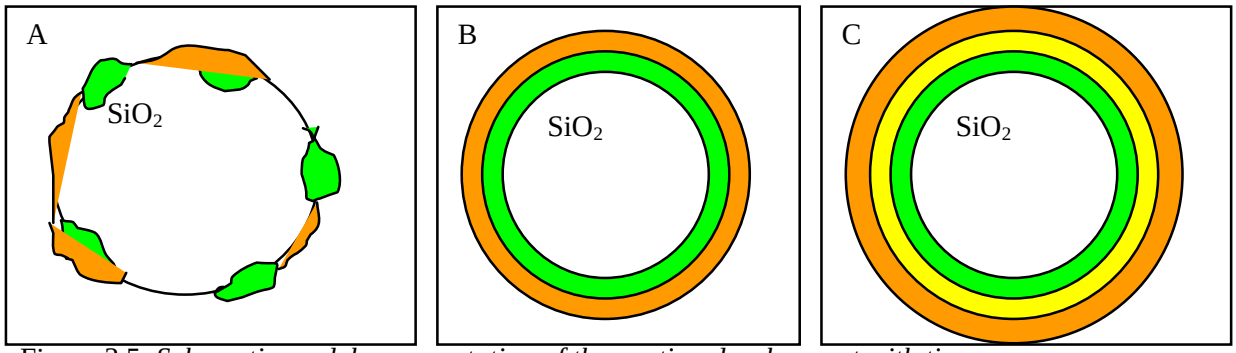

Figure 3.5 *Schematic model representation of the coating development with time*

One of the essential questions in the agglomeration problem due to sintering of coatings, is the origin of the (green) spots of K-silicate reaction zones. The K is from the biomass, the Si, however, could be from the biomass or from the quartz bed material or both. Although no real proof for one or the other origin exists, the following theory is composed from careful and many observations and analyses.

The amount and thickness of the very early K-silicate spots seems to be to some degree related with the K and Si content of the fuel. However, the early reaction spots have a much lower K-content and it increases with time. Evidence exists clearly that the reaction zone moves into the existing quartz grains and the reaction zone becomes more evenly distributed and on average thicker with time. The attachment/reaction of biomass-related K-silicate with the bed material quartz would be very fast. All the development reactions after the initial K-silicate zones seem to be as slow as the formation of the outer coating and the subsequent differentiation. The most likely processes at the later stages seem to be dominated by solid-state diffusion. The very initial formation of K-silicate reaction zones could, however, be dominated by reaction of the quartz crystal with small particles of K-silicate, which purely originate from the biomass itself.

Why is this important? If the bed material consists of SiO_2 and therefore Si is sufficiently available for reaction with K, why is it then so important if this Si comes from the biomass or from the quartz? If many small particles of K-silicate from biomass react with the quartz, this is a fast process. In contrast to this is the slow diffusion dominated process of coating differentiation in which the K-diffuses to react with the crystalline quartz and leaves behind a more refractory outer coating. If the agglomeration indicator shows that the composition of the biomass would favour the formation of an inner and outer coating, it is thought that the refractory outer coating formation can keep forming at the same velocity as the K-silicate reaction layer. Resulting in no-agglomeration. This delicate balance can however be disturbed if in the early stages quick formation of K-silicate zones are formed due to K-silicate from biomass, because in these spots no refractory layer will be on top. In case the number and sizes of these reaction spots are sufficiently small, then with time the diffusion controlled process will form the layering on top, with the K diffusing to the reaction zones and a refractory layer on top. That is also what is observed, that these initial zones grow bigger with time while a small refractory layer forms on top.

In case the number and size of K-silicate reaction spots is initially very large, then agglomeration is likely to occur before the refractory outer coating can form. This is basically the type 2-agglomeration process (sintering due the formation of a molten ash phase) more than the sintering of coatings (see Figure 2). The initial stage, say the first 8 hours of coating formation, are therefore a crucial period to survive for a fluidising bed. The agglomeration indicator that is considered of importance is the earlier proposed ratio of K/Si related to the agglomeration in the olive stone test. The K/Si determines the stickiness of a K-Si composition (generally more K is a lower melting temperature), but in addition a criterion is necessary that determines if the quantity

of K-silicate is so high that the initially formed K-silicate reaction zones on the quartz could lead to agglomeration.

If the experiment with olive-stone is taken as an example, the characteristic of 100% olive stone could be more crucial than the characteristics of the mixture with Cuijk wood, because the reactions via the gas phase between the components of the 2 fuels seem too slow. Likely the combustion of small olive stone particles results in K-silicate molten droplets that react nearly instantly with the quartz bed material.

As a suggestion for further research the following set of conditions form a third agglomeration indicator, proposed to predict type 2- agglomeration:
If:
K/Si>1 (Si from the fuel, not from the bed and not from attached sand to the fuel, because this is both crystalline quartz)
Plus:
K> 3 g/kg fuel and Si > 2 g/kg fuel
Plus:
K+Si (as oxides)> 50% of the total ash content (once total ash is corrected for attached sand).
Than melt-induced sintering in a quartz bed is likely to occur.

4. CONCLUSIONS AND RECOMMENDATIONS

4.1 Conclusions

- For all the investigated combinations of woody fuels (and mixtures of 75% woody fuels and 25% cocoa bean or olive stone pulp) with quartz sand, two common types of coatings can be recognised. Both types consist of concentric coating layers, the number increasing with time from one to three. The two types differ with respect to the presence/absence of K in the inner coating layer. For the different fuels, only the fraction of the two coating types differs. For wood clippings, for example, only the type with K in the inner coating layer was found. Thinning wood and uprooted trees show both types of coatings in roughly equal amounts. Industrial sawdust and the Cuijk mix also show both types of coatings, but the type with K in the inner coating layer is more dominant.

- The coating development on quartz sand, both in terms of morphology and chemistry, appears to follow the same paths for all the fuels investigated. The coating thickness increases with time and with increasing ash content of the fuel. The increase with increasing ash content is less than linear.

- The coating build-up on olivine bed material is chemically different from the build-up on quartz sand.
- Combustion experiments in the lab-scale fluidised-bed installation WOB enable an accurate prediction of the *initial* processes in coating build-up and the associated agglomeration potential in full-scale plants. Lab-scale samples and commercial-scale samples obtained from the Cuijk plant show a similar coating build-up, but the average coating thickness is much larger for the commercial-scale samples. This is most likely due to the longer average residence time for the bed material. It has been observed that the coating thickness continues to increase up to 5.8 days average residence time. The chemical similarity between the lab-scale and commercial-scale samples is striking. The only difference is that in the longer duration WOB experiments, the samples start to show some K and S in the outer coating, while the Cuijk samples never show K and S in the outer coating.

- Three agglomeration indicators have been proposed. The first one predicts the formation of alkali-silicates on the bed material, the second one the formation of a refractory outer coating and the third one the agglomeration potential due to an alkali-silicate melt phase. In general, the experimental findings are in agreement with the behaviour predicted by the indicators, but more critical tests have to be conducted to verify their predictive capabilities.

4.2 Recommendations

- For operators of biomass-fired fluidised-bed combustors, it is recommended to pay careful attention to the chemical analyses of the fuels and, as a first approximation, to use the three proposed indicators for the assessment of their agglomeration potential.

- Specifically for the Cuijk situation, when taking the differences between summer and winter fuels into account, the bed material renewal rate when using winter fuels could be lower, saving money on the amount of used sand. Or alternatively, the fraction of wood clippings could be larger in wintertime, saving money on fuel costs. In addition, the difference between the alternative fuels, cocoa bean and olive stone pulp, and the summer

fuel mix appears limited. If the alternative fuels are less expensive, then their use as (partial) replacement for the summer fuels seems an interesting option.

- Further research is recommended to further elucidate the mechanisms of the agglomeration process. In particular, this should include the following:
  - To model and experimentally test a broader range of fuels. From the samples to be studied by SEM/EDX it must be possible to elucidate whether the proposed agglomeration indicators can be used to assess the agglomeration potential.
  - The experiment with olivine as bed material shows that the type of coating build-up with time is chemically different from that on quartz sand. In future research, olivine and other alternative bed materials may be considered in more detail to arrive at optimum strategies for minimising the agglomeration potential.

5. REFERENCES

[1] Visser, H.J.M., Lith, S.C. van, and Kiel, J.H.A.: Biomass Ash - Bed Material Interactions Leading to Agglomeration in FBC. Proceedings of FBC-17: 17th International Conference on Fluidised-bed Combustion, May 18-21, 2003, Jacksonville, Florida.

[2] Final Report EU project "Improved Energy Generation Based on Biomass FBC with Minimum Emissions". Contract No. JOR3-CT98-0200, Oct. 1998 - Sept. 2000.

[3] Visser, H.J.M., Hofmans, H., Huijnen, H., Kastelein, R. and Kiel, J.H.A.: Biomass ash – bed material interaction leading to agglomeration in fluidised bed combustion and gasification. In: Progress in Thermochemical Biomass Conversion, Vol 1. Ed A.V. Bridgwater. Blackwell Science, 2001.

[4] Laitinen, R., Nuutinen, L., Tiainen, M., and Virtanen, M.: An improved bed material for the BFB-boilers. Case 2: Combustion of fuel with high Na content. Proc. 5th European conf. on Industrial Furnaces and Boilers, Porto, Portugal, 11-14 April 2000.

[5] Lind, T., Valmari, T., Kauppinen, E., Nilsson, K., Sfiris, G., and Maenhaut, W.: Ash formation mechanisms during combustion of wood in circulating fluidised beds. Proceedings of the 28th international symposium on combustion, Edingborough, 30 July - 4 August 2000.

[6] Öhman, M., Nordin, A., Skrivars, B.-J., Backman, R., and Hupa, M.: Bed agglomeration characteristics during fluidised bed combustion of biomass. Energy & Fuels 14, p169-178, 2000.

[7] Heemskerk, G.C.A.M.: Best Practice List for Biomass Fuel and Ash Analysis. KEMA report 95026-KPG/TCM-98-7003, 1998

[8] EU-project "Biomass/Waste Fluidised Bed Combustion with Inorganics Control (BIFIC)". Contract ENK-5-CT-2000-00335, Feb. 2001 - Jan. 2004.

APPENDIX 1 FUELS

Table 1. Per fuel are shown, the heating value, proximate en ultimate analyses and analyses of the main inorganic elements as determined by ICP/AES.

Fuel/ analysis	Wood clippings 1	Wood clippings 2	Uprooted trees 1	Uprooted trees 2	Thinning wood 1	Thinning wood 2	Saw dust 1	Saw dust 2	Cuijk-Mix1* analysed	Cuijk-Mix2* analysed	Cuijk-mix1* calculated)+	Cuijk-mix2* calculated)+	Olive-stone pulpe	Cacao beans
Heating value (HHV in J/g)	19960	17230	19936	19250	19500	20009	20430	20587	20320	19956	20256	20110	17100	24355
Ash content (550°C) (%)	2.75	17.0	1.79	7.1	0.86	4.85	0.60	0.73	0.94	3.79	0.84	3.17	6.2	5.2
Moisture content (%)	5.5	3.0	4.7	4.5	3.6	3.2	4.3	0.4	5.1	3.0	4.37	3	10.3	6.5
Vluchtig gehalte (%)	77.4	62.79	79.9	72.0	80.8	74.1	81.5	81.7	81.1	76.6	80.9	78.4		
C (dry)	48.3	41.6	47.6	47.1	49.3	48.1	48.5	49.0	48.1	48.3	48.1	48.1	55.28	58.7
H (dry)	5.73	5.05	5.86	5.72	5.95	5.96	5.88	6.02	6.0	6.1	6	5.9	5.28	8.8
O (dry)	42.8	37.06	43.0	41.9	42.7	43.5	45.2	44.0	43.9	44.2	43.9	43.13	38.11	29.7
N (dry)	0.31	0.70	0.31	0.66	0.22	0.49	0.10	0.11	0.17	0.25	0.2	0.24	1.33	2.8
Cl (g/kg)	0.143	0.994	0.125	0.278	0.073	0.234	<0.400	0.048	<0.330	0.191	0.323	0.176	1.3	1
S (g/kg)	0.290	0.787	0.278	0.613	0.194	0.467	0.103	0.106	0.128	0.300	0.142	0.242	0.325	3.1
Si (g/kg)	12.870	60.239	0.250	12.660	0.089	5.038	0.072	0.133	0.134	12.208	1.364	7.410	2.751	0.148
Al (g/kg)	0.550	3.511	0.059	0.706	0.048	0.361	0.023	0.050	0.043	0.430	0.080	0.468	0.195	0.015
Na (g/kg)	0.324	0.946	0.108	0.242	0.053	0.245	0.031	0.033	0.045	0.147	0.067	0.159	0.122	0.107
K (g/kg)	2.300	5.048	1.791	3.156	1.169	2.999	0.796	0.666	0.983	1.752	1.045	1.499	3.399	4.166
Ca (g/kg)	4.375	9.413	3.451	9.882	1.863	7.727	1.343	1.4263	1.578	3.690	1.827	3.394	5.529	1.698
Mg (g/kg)	0.522	1.048	0.407	0.763	0.276	0.622	0.173	0.166	0.222	0.365	0.233	0.338	1.407	2.061
P (g/kg)	0.316	0.819	0.389	0.725	0.193	0.580	0.095	0.085	0.145	0.321	0.145	0.249	0.153	0.716
Fe (g/kg)	0.815	2.347	0.213	1.226	0.097	0.535	0.143	0.141	0.198	0.838	0.210	0.468	0.200	0.044
Mn (g/kg)	0.044	0.132	0.037	0.065	0.045	0.040	0.086	0.083	0.088	0.068	0.075	0.082	0.040	0.04
Cr (g/kg)	0.008	0.018	0.001	0.005	0.001	0.002	0.001	0.001	0.001	0.006	0.002	0.003	0.016	0.015

* Cuijk-mix consists of: 10% wood clippings, 6% uprooted trees, 10.5% thinning wood and 73.5% saw dust

+ The calculated Cuijkmix is based on the analyses of the individual streams in the mix, multiplied by their percentage in de mix.